LIFETIMES OF QUASIPARTICLES

AND COLLECTIVE EXCITATIONS

IN HOT QED PLASMAS

Jean-Paul BLAIZOT[*] and Edmond IANCU[†]

Service de Physique Théorique[‡], CE-Saclay

91191 Gif-sur-Yvette, France

Abstract

The perturbative calculation of the lifetime of fermion excitations in a QED plasma at high temperature is plagued with infrared divergences which are not eliminated by the screening corrections. The physical processes responsible for these divergences are the collisions involving the exchange of longwavelength, quasistatic, magnetic photons, which are not screened by plasma effects. The leading divergences can be resummed in a non-perturbative treatement based on a generalization of the Bloch-Nordsieck model at finite temperature. The resulting expression of the fermion propagator is free of infrared problems, and exhibits a *non-exponential* damping at large times: $S_R(t) \sim \exp\{-\alpha T\, t \ln \omega_p t\}$, where $\omega_p = eT/3$ is the plasma frequency and $\alpha = e^2/4\pi$.

---

[*]CNRS

[†]CNRS

[‡]Laboratoire de la Direction des Sciences de la Matière du Commissariat à l'Energie Atomique

1 Introduction

The study of the elementary excitations of ultrarelativistic plasmas, such as the quark-gluon plasma, has received much attention in the recent past [1—11] (See also [12, 13] for recent reviews and more references.) The physical picture which emerges is that of a system with two types of degrees of freedom: *i*) the plasma quasiparticles, whose energy is of the order of the temperature T; *ii*) the collective excitations, whose typical energy is gT, where g is the gauge coupling, assumed to be small: $g \ll 1$ (in QED, $g = e$ is the electric charge). For this picture to make sense, however, it is important that the lifetime of the excitations be large compared to the typical period of the modes.

Information about the lifetime is obtained from the retarded propagator. A usual expectation is that $S_R(t, \mathbf{p})$ decays *exponentially* in time, $S_R(t, \mathbf{p}) \sim \mathrm{e}^{-iE(p)t}\mathrm{e}^{-\gamma(p)t}$, so that $|S_R(t, \mathbf{p})|^2 \sim \mathrm{e}^{-\Gamma(p)t}$ with $\Gamma(p) = 2\gamma(p)$, which identifies the lifetime of the single particle excitation as $\tau(p) = 1/\Gamma(p)$. The exponential decay may then be associated to a pole of the Fourier transform $S_R(\omega, \mathbf{p})$, located at $\omega = E(p) - i\gamma(p)$. The quasiparticles are well defined if their lifetime τ is much larger than the period $\sim 1/E$ of the field oscillations, that is, if the damping rate γ is small compared to the energy E. If this is the case, the respective damping rates can be computed from the imaginary part of the on-shell self-energy, $\Sigma(\omega = E(p), \mathbf{p})$. Such calculations suggest that $\gamma \sim g^2 T$ [3, 4] for both the single-particle and the collective excitations. In the weak coupling regime $g \ll 1$, this is indeed small compared to the corresponding energies (of order T and gT, respectively), suggesting that the quasiparticles are well defined, and the collective modes are weakly damped. However, the computation of γ in perturbation theory is plagued with infrared divergences, which casts doubt on the validity of these statements [3], [15—26]

The first attempts to calculate the damping rates were made in the early 80's. It was then found that, to one-loop order, the damping rate of the soft collective excitations in the hot QCD plasma was gauge-dependent, and could turn out negative in some gauges (see Ref. [27] for a survey of this problem). Decisive progress on this problem was made by Pisarski [3] and Braaten and Pisarski who identified the resummation needed to obtain the screening corrections in a gauge-invariant way [4] (the resummation of the so called "hard thermal loops" (HTL)). Such screening corrections are sufficient to make finite the transport cross-sections[6, 7], and also the damping rates of excitations with zero momentum[4, 8]. At the same time, however, it has been remarked[3] that the HTL

resummation is not sufficient to render finite the damping rates of excitations with non vanishing momenta. The remaining infrared divergences are due to collisions involving the exchange of longwavelength, quasistatic, magnetic photons (or gluons), which are not screened in the hard thermal loop approximation. Such divergences affect the computation of the damping rates of *charged* excitations, in both abelian and non-abelian gauge theories. Thus, in the lowest order calculations of Refs. [3], [15—26], one meets the same logarithmic divergence for electrons in QED, for charged scalars in SQED, and for quarks and gluons in QCD. (There is no such problem for the photon damping rate, which is IR finite and of order g^4T [28], since photons do not couple directly to gluons or to themselves.) Furthermore, the problem appears for both soft ($p \sim gT$) and hard ($p \sim T$) quasiparticles. In QCD this problem is generally avoided by the *ad-hoc* introduction of an IR cut-off ("magnetic screening mass") $\sim g^2T$, which is expected to appear dynamically from gluon self-interactions [29]. In QED, on the other hand, it is known that no magnetic screening can occur[30], so that the solution of the problem must lie somewhere else.

In order to make the damping rate γ finite, Lebedev and Smilga proposed a self-consistent computation of the damping rate γ[15], by including γ also in internal propagators. However, the resulting self-energy is not analytic near the complex mass-shell, and the logarithmic divergence actually reappears when the discontinuity of the self-energy is evaluated at $\omega = E - i\gamma$ [17, 18]. More thorough resummations of the fermion line led to the conclusion that the full fermion propagator has actually no quasiparticle pole in the complex energy plane[23, 21]. These analyses left unanswered, however, the question of the large time behavior of the retarded propagator. As we have shown in a previous letter[31], the answer to this question requires resummations for both the fermion propagator and the photon-electron vertex function. Such resummations modify the analytic structure of the retarded propagator: indeed, as we shall see, they make it analytic in the vicinity of the mass-shell.

The need for a nonperturbative analysis follows from the fact that infrared divergences occur in *all* orders of perturbation theory. The *leading* divergences arise, in all orders, from the same kinematical regime as in the one loop calculation, namely from the exchange of soft *quasistatic* magnetic photons. In the imaginary time formalism, these divergences are concentrated in diagrams in which the photon lines carry zero Matsubara frequency (to be referred as *static modes* in what follows). In this sense, they appear as the divergences of an effective three-dimensional gauge theory, which is intrinsically non-

perturbative. Still, this effective "dimensional reduction" brings in simplifications which can be exploited to arrive at an explicit solution of the problem.

We concentrate in this paper on the damping rate of fermionic excitations in hot QED plasmas. Our analysis is based on the Bloch-Nordsieck (or eikonal) approximation[32]. At zero temperature, this approximation provides an all-order solution to the infrared catastrophe, and correctly describes the mass-shell structure of the 4-dimensional fermion propagator[33]. At finite temperature, the Bloch-Nordsieck approximation has been previously used, by Weldon, to verify the cancellation of the infrared divergences in the production rate for soft real photons [34]. Let us also mention that an attempt to solve the IR problem of the damping rate, using the BN approximation in the same spirit as in the present paper, has been reported in Ref. [35]. However, although the final result obtained in [35] is similar to ours, the derivations there are plagued with several inconsistencies, some of which are pointed out in [31].

In this paper, we shall consider (in section 3) a different generalization of the Bloch-Nordsieck (BN) model at finite temperature, which is better suited to study the infrared structure of the fermion propagator. Our approach is a natural extension of the method used in Ref. [33] in QED_{3+1} at zero temperature. However, the resulting imaginary-time BN propagator does not exponentiate in an obvious way, and thus cannot be written in closed form, in contrast to the usual, zero-temperature propagator. Still, we can obtain an explicit solution once we restrict ourselves to the static Matsubara photon modes. We thus get the retarded propagator $S_R(t, \mathbf{p})$, and study its large time behavior (section 4). The final result is that, for times $t \gg 1/gT$, the propagator does not show the usual exponential decay alluded to before, but the more complicated behavior $S_R(t, \mathbf{p}) \sim e^{-iE(p)t} e^{-\alpha T t \ln \omega_p t}$, where $\omega_p \sim gT$ is the plasma frequency, and $E(p) \simeq p \sim T$ is the average energy of the hard fermion. This corresponds to a typical lifetime $\tau^{-1} \sim g^2 T \ln(1/g)$, which is similar to the one provided by the perturbation theory with an IR cut-off of the order $g^2 T$. Since, as $t \to \infty$, $S_R(t)$ is decreasing faster than any exponential, the Fourier transform of $S_R(t, \mathbf{p})$, $S_R(\omega, \mathbf{p})$, is an entire function in the complex energy plane. The existence of the quasiparticle is therefore not signaled by the presence of a pole of $S_R(\omega)$ in the complex energy plane. However, the associated spectral density has the shape of a *resonance* strongly peaked around $\omega = E(p)$, with a typical width of the order $1/\tau \sim g^2 T \ln(1/g)$. With minor modifications, the above conclusions also apply for the *soft* (collective) excitations, with momenta $p \sim gT$, whose lifetimes are found to depend

3

on the group velocities $|v_\pm| < 1$ (section 5).

At this stage it is useful to specify the notations and the conventions to be used throughout. The analytic propagator is defined in the complex energy plane by the spectral representation

$$S(\omega, \mathbf{p}) = \int_{-\infty}^{+\infty} \frac{dp^0}{2\pi} \frac{\rho_f(p^0, \mathbf{p})}{p^0 - \omega}. \tag{1.1}$$

The Matsubara propagator is obtained from eq. (1.1) by setting $\omega = i\omega_n$, with $\omega_n = (2n+1)\pi T$ and integer n. At tree level, $\rho_f(p^0, \mathbf{p}) = \not{p}\rho_0(p^0, p)$ where $\not{p} = p^\mu\gamma_\mu$, $\epsilon_p \equiv |\mathbf{p}| = p$, and

$$\rho_0(p^0, p) = \frac{\pi}{\epsilon_p}\left(\delta(p^0 - \epsilon_p) - \delta(p^0 + \epsilon_p)\right), \tag{1.2}$$

so that

$$S_0(\omega, \mathbf{p}) = -\frac{\omega\gamma^0 - \mathbf{p}\cdot\boldsymbol{\gamma}}{\omega^2 - p^2} = \frac{-1}{\omega - p}h_+(\hat{\mathbf{p}}) + \frac{-1}{\omega + p}h_-(\hat{\mathbf{p}}), \tag{1.3}$$

where $h_\pm(\hat{\mathbf{p}}) = (\gamma^0 \mp \hat{\mathbf{p}}\cdot\boldsymbol{\gamma})/2$, with $\hat{\mathbf{p}} \equiv \mathbf{p}/p$.

The full fermion propagator is given by the Dyson-Schwinger equation

$$S^{-1}(\omega, \mathbf{p}) = S_0^{-1}(\omega, \mathbf{p}) + \Sigma(\omega, \mathbf{p}). \tag{1.4}$$

The most general form of the self-energy Σ which is compatible with the rotational and chiral symmetries is

$$\Sigma(\omega, \mathbf{p}) = a(\omega, p)\gamma^0 + b(\omega, p)\hat{\mathbf{p}}\cdot\boldsymbol{\gamma} \equiv h_-(\hat{\mathbf{p}})\Sigma_+(\omega, p) - h_+(\hat{\mathbf{p}})\Sigma_-(\omega, p), \tag{1.5}$$

where

$$\Sigma_\pm(\omega, p) = \pm\frac{1}{2}\operatorname{tr}\left(h_\pm(\hat{\mathbf{p}})\Sigma(\omega, \mathbf{p})\right). \tag{1.6}$$

Using this decomposition of Σ onto $h_\pm$, and the analogous one for S_0, eq. (1.3), one can easily invert eq. (1.4) to get the full propagator:

$$S(\omega, \mathbf{p}) = \Delta_+(\omega, p)h_+(\hat{\mathbf{p}}) + \Delta_-(\omega, p)h_-(\hat{\mathbf{p}}), \tag{1.7}$$

where

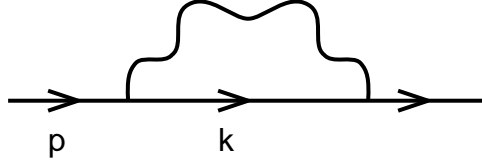$$\Delta_\pm(\omega, p) = \frac{-1}{\omega \mp (p + \Sigma_\pm(\omega, p))}. \tag{1.8}$$

4

Figure 1: The one-loop fermion self-energy

The retarded propagator is obtained as the boundary value of the analytic propagator (1.1) when ω approaches the real axis from above, i.e., $S_R(\omega, \mathbf{p}) = S(\omega + i\eta, \mathbf{p})$, where ω is real and $\eta \to 0_+$. In the time representation,

$$S_R(t, \mathbf{p}) = \int_{-\infty}^{\infty} \frac{d\omega}{2\pi} e^{-i\omega t} S_R(\omega, \mathbf{p}) = i\theta(t) \int_{-\infty}^{\infty} \frac{d\omega}{2\pi} e^{-i\omega t} \rho_f(\omega, \mathbf{p}). \tag{1.9}$$

The large time behavior of $S_R(t, \mathbf{p})$ is determined by the analytic structure of $S_R(\omega, \mathbf{p})$ when continued to complex values of ω. In the upper half plane, $S_R(\omega)$ coincides with the analytic propagator (1.1). In the lower half plane, $S_R(\omega)$ is defined by continuation across the real axis, and it may have there singularities. The large time behavior of $S_R(t)$ is controlled in most cases by the singularity of $S_R(\omega)$ which lies closest to the real axis. If this is located at $\omega = E(p) - i\gamma(p)$, then $S_R(t, \mathbf{p}) \sim f(t, \mathbf{p}) e^{-iE(p)t} e^{-\gamma(p)t}$, where the prefactor $f(t, \mathbf{p})$ is slowly varying, and depends on the specific nature of the singularity. This conventional picture breaks down in gauge theories since, as we shall discuss in the next section, the perturbative estimate of γ turns out to be IR divergent. The resummation of the leading infrared divergences, carried out in section 3, produces a propagator which has no singularity in the complex ω plane. We shall then find it convenient to calculate $S_R(t)$ directly, rather than from the Fourier transform (1.9).

2 The one-loop damping rate for the hard fermion

In this section, we review the perturbative calculations of the damping rate for a hard fermion, with momentum $p \sim T$ [15—26] focussing on the infrared divergences which arise in such calculations. We assume here, as customary, that the dominant singularity of the retarded propagator is a simple pole whose location goes back into the tree-level pole at $\omega = p$ when $g \to 0$.
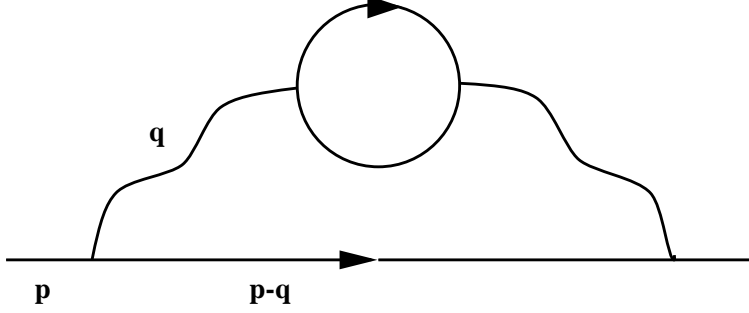
Figure 2: Two-loop diagram contributing to the fermion self-energy

2.1 Physical interpretation of the damping

To leading order in g, the self-energy is given by the one-loop diagram in Fig. 1. This gives no contribution to the damping rate γ. Indeed, when evaluated on the free mass-shell, i.e. at $\omega = p$, the imaginary part of the one-loop self-energy vanishes because of kinematics. (At finite temperature this argument involves subtleties which are discussed in Appendix B.)

The leading contribution to γ comes therefore from the two-loop diagram in Fig. 2, and turns out to be quadratically infrared divergent (see, e.g., Refs. [6, 7, 19, 13]).

The on-shell imaginary part is obtained by cutting the diagram in Fig. 2 through the internal fermion loop and the lower fermion propagator. Physically, this imaginary part accounts for the scattering of the incoming electron (with four momentum $p^\mu = (\epsilon_p, \mathbf{p})$ and $\epsilon_p = p$) off a thermal fermion (electron or positron), calculated in the Born approximation (see Fig. 3). The total interaction rate is given by

$$\begin{aligned}
\Gamma(p) &= \frac{1}{2\epsilon} \int d\tilde{p}_1 \, d\tilde{p}_2 \, d\tilde{p}_3 \, (2\pi)^4 \delta^{(4)}(p + p_1 - p_2 - p_3) \\
&\quad \left\{ n_1(1 - n_2)(1 - n_3) + (1 - n_1)n_2 n_3 \right\} |\mathcal{M}|^2,
\end{aligned} \quad (2.1)$$

and coincides with twice the damping rate $\gamma(p)$, as computed from the two-loop self-energy in Fig. 2: $\Gamma(p) = 2\gamma(p)$. This identity extends to finite temperature the usual physical interpretation of the self-energy discontinuity in terms of cross-sections for physical processes, and can be verified through an explicit calculation[13] (see also below). The notations in eq. (2.1) are as follows: all the particles are on the mass-shell (i.e., $\epsilon = p$ and $\epsilon_i = p_i$ for $i = 1, 2, 3$), and we have denoted $\int d\tilde{p}_i \equiv \int (d^3 p_i/(2\pi)^3 \, 2\epsilon_i)$. The factors $n_i = n(\epsilon_i)$ are the thermal occupation numbers for fermions $(n(\epsilon) = 1/(e^{\beta\epsilon} + 1))$. Note that, for fermions, the rates of the direct and of the reverse processes have to be *added* to
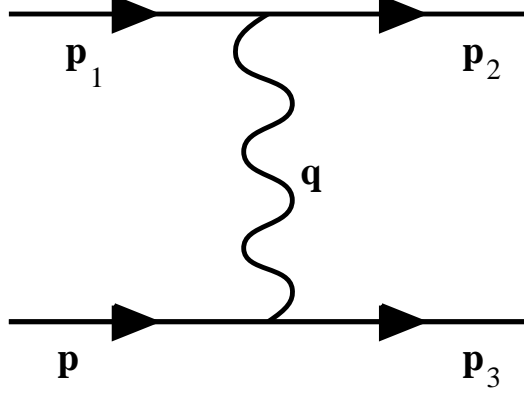
Figure 3: Fermion-fermion elastic scattering in the Born approximation

give the total depopulation of the fermion state with momentum p^μ [14]. Finally, $|\mathcal{M}|^2$ is the scattering matrix element squared, averaged over the spin s of the incoming electron, and summed over the spins s_1, s_2 and s_3 of the other three particles. In the Born approximation, $|\mathcal{M}|^2$ is independent of the temperature and involves the propagator $D_{\mu\nu}(q)$ of the exchanged photon (with $q = p - p_3 = p_2 - p_1$). Specifically[38],

$$|\mathcal{M}|^2 = 16g^4 D_{\mu\nu}(q) D^*_{\rho\lambda}(q) \left\{ p^\mu p_3^\rho + p_3^\mu p^\rho - g^{\mu\rho}(p \cdot p_3) \right\} \left\{ p_1^\nu p_2^\lambda + p_2^\nu p_1^\lambda - g^{\nu\lambda}(p_1 \cdot p_2) \right\}. \quad (2.2)$$

We shall use below the Coulomb gauge where the only non-trivial components of $D_{\mu\nu}(q)$ are the electric (or longitudinal) one $D_{00}(q) \equiv \Delta_l(q)$, and the magnetic (or transverse) one $D_{ij}(q) = (\delta_{ij} - \hat{q}_i\hat{q}_j)\Delta_t(q)$.

Since the interaction rate (2.1) is dominated by soft momentum transfers $q \ll T$, while the external momenta are typically of the order of T, we can simplify the matrix element $|\mathcal{M}|^2$ by setting $\mathbf{p} \simeq \mathbf{p_3}$ and $\mathbf{p_1} \simeq \mathbf{p_2}$ in eq. (2.2), and obtain

$$|\mathcal{M}|^2 \simeq 64g^4 p^2 p_1^2 \left| \Delta_l(q) + (\mathbf{v} \times \hat{\mathbf{q}}) \cdot (\mathbf{v_1} \times \hat{\mathbf{q}}) \Delta_t(q) \right|^2, \quad (2.3)$$

with $\mathbf{v} \equiv \hat{\mathbf{p}}$ and $\mathbf{v_1} \equiv \hat{\mathbf{p_1}}$. Furthermore, we use energy conservation to write $q_0 = \epsilon - \epsilon_3 = \epsilon_2 - \epsilon_1$, that is,

$$q_0 = p - |\mathbf{p} - \mathbf{q}| = |\mathbf{p_1} + \mathbf{q}| - p_1,$$

which, for $q \ll T$, becomes

$$q_0 \simeq \mathbf{v} \cdot \mathbf{q} \simeq \mathbf{v_1} \cdot \mathbf{q}. \quad (2.4)$$

The statistical factors in eq. (2.1) satisfy the following identity:

$$n_1(1 - n_2)(1 - n_3) + (1 - n_1)n_2 n_3 = (n_1 - n_2)(1 + N(q_0) - n_3), \quad (2.5)$$

7

which features $N(q_0)$, the Bose-Einstein thermal factor for the virtual photon. Since $\epsilon_2 = \epsilon_1 + q_0$, and $q_0 \ll p_1 \sim T$,

$$(n_1 - n_2)(1 + N(q_0) - n_3) \simeq -\frac{\mathrm{d}n}{\mathrm{d}p_1} q_0 N(q_0) \simeq -T\frac{\mathrm{d}n}{\mathrm{d}p_1}, \tag{2.6}$$

where we have used the fact that, at small $q_0 \ll T$,

$$1 + N(q_0) - n_3 \simeq N(q_0) \simeq T/q_0. \tag{2.7}$$

Finally, we use eq. (2.4) to rewrite the integrations over $\mathbf{p_2}$ and $\mathbf{p_3}$ as follows

$$\int \frac{\mathrm{d}^3 p_2}{(2\pi)^3} \int \frac{\mathrm{d}^3 p_3}{(2\pi)^3} (2\pi)^4 \delta^{(4)}(p + p_1 - p_2 - p_3)$$
$$= \int \frac{\mathrm{d}^3 q}{(2\pi)^3} \int_{-\infty}^{\infty} \frac{\mathrm{d}q_0}{2\pi} 2\pi\delta(q_0 - \mathbf{v} \cdot \mathbf{q}) 2\pi\delta(q_0 - \mathbf{v_1} \cdot \mathbf{q}), \tag{2.8}$$

so that we may use $\mathbf{p_1}$, $\mathbf{q}$ and q_0 as independent integration variables in eq. (2.1):

$$\Gamma(p) \simeq 16\pi^2 g^4 T \int \frac{\mathrm{d}^3 p_1}{(2\pi)^3} \left(-\frac{\mathrm{d}n}{\mathrm{d}p_1}\right) \int \frac{\mathrm{d}^3 q}{(2\pi)^3} \int_{-\infty}^{\infty} \frac{\mathrm{d}q_0}{2\pi}$$
$$\delta(q_0 - \mathbf{v} \cdot \mathbf{q}) \, \delta(q_0 - \mathbf{v_1} \cdot \mathbf{q}) \left|\Delta_l(q) + (\mathbf{v} \times \hat{\mathbf{q}}) \cdot (\mathbf{v_1} \times \hat{\mathbf{q}})\Delta_t(q)\right|^2. \tag{2.9}$$

We perform the angular integrations over $\mathbf{v_1} \equiv \hat{\mathbf{p}}_1$ and $\hat{\mathbf{q}}$ by using the delta functions, while the radial integration over p_1 gives

$$\int \mathrm{d}p_1 p_1^2 \left(-\frac{\mathrm{d}n}{\mathrm{d}p_1}\right) = \frac{\pi^2 T^2}{6}. \tag{2.10}$$

We obtain finally

$$\Gamma \simeq \frac{g^4 T^3}{6} \int_0^{q^*} \mathrm{d}q \int_{-q}^{q} \frac{\mathrm{d}q_0}{2\pi} \left\{ |\Delta_l(q_0, q)|^2 + \frac{1}{2}\left(1 - \frac{q_0^2}{q^2}\right)^2 |\Delta_t(q_0, q)|^2 \right\}, \tag{2.11}$$

where the upper cut-off q^* distinguishes between soft and hard momenta: $gT \ll q^* \ll T$. Since the q-integral is dominated by IR momenta, its leading order value is actually independent of q^*.

The two terms within the parentheses in eq. (2.11) correspond to the exchange of an electric and of a magnetic photon respectively. For a bare photon, we have $|\Delta_l(q_0, q)|^2 = 1/q^4$ and $|\Delta_t(q_0, q)|^2 = 1/(q_0^2 - q^2)^2$, so that the q-integral in eq. (2.11) shows a quadratic IR divergence:

$$\Gamma \simeq \frac{g^4 T^3}{4\pi} \int_0^{q^*} \frac{\mathrm{d}q}{q^3}. \tag{2.12}$$

This divergence reflects the singular behaviour of the Rutherford cross-section for forward scattering [38].

As well known, however, the quadratic divergence is removed by the screening corrections contained in the photon polarization tensor. These modify the electric and magnetic propagators as follows

$$
{}^*\Delta_l(q_0, q) = \frac{-1}{q^2 - \delta\Pi_l(q_0, q)}, \qquad {}^*\Delta_t(q_0, q) = \frac{-1}{q_0^2 - q^2 - \delta\Pi_t(q_0, q)}, \qquad (2.13)
$$

where $\delta\Pi_l$ and $\delta\Pi_t$ are the respective pieces of the photon polarisation tensor (in the hard thermal loop approximation[1, 2]). We shall see below that the leading IR contribution comes from the domain $q_0 \ll q \ll T$, where we can use the approximate expressions

$$
\delta\Pi_l(q_0 \ll q) \simeq 3\omega_p^2 \equiv m_D^2, \qquad \delta\Pi_t(q_0 \ll q) \simeq -i\,\frac{3\pi}{4}\,\omega_p^2\,\frac{q_0}{q}\,. \qquad (2.14)
$$

We see that screening occurs in different ways in the electric and the magnetic sectors. In the electric sector, the familiar static Debye screening provides an IR cut-off $m_D \sim gT$. Accordingly, the electric contribution to Γ is finite, and of the order $\Gamma_l \sim g^4 T^3/m_D^2 \sim g^2 T$. Its exact value can be computed by numerical integration[18]. In the magnetic sector, screening occurs only for nonzero frequency q_0 [2, 6]. This comes from the imaginary part of the polarisation tensor, and can be associated to the Landau damping of space-like photons ($q_0^2 < q^2$). This "dynamical screening" is not sufficient to completely remove the IR divergence of Γ_t:

$$
\begin{aligned}
\Gamma_t &\simeq \frac{g^4 T^3}{12} \int_0^{q^*} \mathrm{d}q \int_{-q}^{q} \frac{\mathrm{d}q_0}{2\pi} \frac{1}{q^4 + (3\pi\omega_p^2 q_0/4q)^2} \\
&= \frac{g^2 T}{\pi^2} \int_0^{q^*} \frac{\mathrm{d}q}{q} \arctan\left(\frac{3\pi\omega_p^2}{4q^2}\right) \simeq \frac{g^2 T}{2\pi} \int_0^{\omega_p} \frac{\mathrm{d}q}{q}\,.
\end{aligned} \qquad (2.15)
$$

In writing the last equality, we payed attention only to the dominant, logarithmically divergent, contribution. To isolate it, we have written

$$
\arctan\left(\frac{3\pi\omega_p^2}{4q^2}\right) \simeq \frac{\pi}{2}\,,
$$

as appropriate for $q \ll \omega_p$, and we have introduced the upper cut-off $\omega_p \sim gT$ to approximately account for the correct UV behaviour of the integrand: namely, as $q \gg \omega_p$, the integrand is decreasing like ω_p^2/q^3, so that the q-integral is indeed cut-off at $q \sim \omega_p$.

The remaining IR divergence in eq. (2.15) is due to collisions involving the exchange of very soft ($|\mathbf{q} \to \mathbf{0}|$), *quasistatic* ($q_0 \to 0$) magnetic photons, which are not screened by

plasma effects. To see that, note that the IR contribution to Γ_t comes from momenta $q \ll gT$, where $|\Delta_t(q_0, q)|^2$ is almost a delta function of q_0:

$$|\Delta_t(q_0, q)|^2 \simeq \frac{1}{q^4 + (3\pi\omega_p^2 q_0/4q)^2} \xrightarrow{q \to 0} \frac{4}{3q\omega_p^2} \delta(q_0) \,. \tag{2.16}$$

This is so because, as $q_0 \to 0$, the imaginary part of the polarisation tensor vanishes *linearly* (see the second equation (2.14)), a property which can be related to the behaviour of the phase space for the Landau damping processes. Since energy conservation requires $q_0 = q \cos\theta$, where θ is the angle between the momentum of the virtual photon ($\mathbf{q}$) and that of the incoming fermion ($\mathbf{p}$), the magnetic photons which are responsible for the singularity are emitted, or absorbed, at nearly 90 degrees.

To conclude this subsection, we note that, if we temporarily leave aside the logarithmic divergence, then both the electric and the magnetic damping rates are of order $g^2 T$, rather than $g^4 T$ as one would naively expect by looking at the diagrams in Figs. 2 and 3. This situation has been sometimes referred as *anomalous damping* [15], and is a consequence of the strong sensitivity of the scattering cross section to the IR behavior of the photon propagator. By comparison, the other two-body collisions leading to the damping of the fermion, namely the Compton scattering and the annihilation process, are less IR singular — as they involve the exchange of a virtual *fermion* — and only contribute at order $g^4 T$.

2.2 Resummed one-loop self-energy

While the above calculation of the interaction rate in the Born approximation is physically transparent, for the subsequent developments in this paper it is more convenient to obtain γ from the imaginary part of the self-energy. To lowest order, we can write $\gamma(p) = -\mathrm{Im}\,\Sigma_+(p, p)$, with $\Sigma_+(\omega, p)$ defined as in eq. (1.6) in terms of the *resummed* one-loop self-energy. The corresponding diagram is displayed in Fig. 4: the blob on the photon line in this figure denotes the effective photon propagator of eq. (2.13).

To evaluate the one-loop diagram in Fig. 4, we use the imaginary time formalism and write

$$\Sigma(p) \;=\; -g^2 T \sum_{q^0 = i\omega_m} \int \frac{\mathrm{d}^3 q}{(2\pi)^3} \, \gamma_\mu \, S_0(p - q) \, \gamma_\nu \, {}^*D^{\mu\nu}(q) \,. \tag{2.17}$$

In this equation, all the energy variables are purely imaginary and discrete to start with; namely, $p^0 = i\omega_n = i(2n + 1)\pi T$ for the external fermion line, and $q^0 = i\omega_m = i2\pi mT$
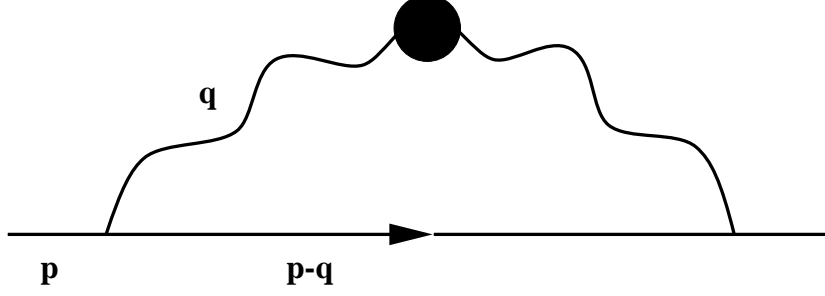
10

Figure 4: The resummed one-loop self-energy

for the internal photon line, with integers n and m. Furthermore, $\mathbf{k} = \mathbf{p} - \mathbf{q}$, $S_0(p-q)$ is the free fermion propagator, eq. (1.3), and $^*D^{\mu\nu}(q)$ is the resummed photon propagator. We shall perform our computations in the Coulomb gauge (the one-loop damping rate is gauge independent[4, 39, 40]; see also Appendix B).

The continuation of $\Sigma(p)$ to real external energy can be done only *after* performing the Matsubara sum over $q_0 = i\omega_m$, and consists in simply replacing (for retarded boundary conditions) $p^0 = i\omega_n$ by $\omega + i\eta$, with real ω and $\eta \to 0_+$. In order to perform the Matsubara sum in eq. (2.17), it is convenient to use the spectral representations of the various propagators. For S_0, this is given in eq. (1.1), with $\rho_f(p^0, \mathbf{p}) = \not{p}\rho_0(p^0, p)$. For the electric and magnetic photon propagators we have similarly

$$
\begin{aligned}
{}^*\Delta_t(\omega, \mathbf{q}) &= \int_{-\infty}^{\infty} \frac{\mathrm{d}q_0}{2\pi} \frac{{}^*\rho_t(q_0, q)}{q_0 - \omega}, \\
{}^*\Delta_l(\omega, \mathbf{q}) &= -\frac{1}{q^2} + \int_{-\infty}^{\infty} \frac{\mathrm{d}q_0}{2\pi} \frac{{}^*\rho_l(q_0, q)}{q_0 - \omega},
\end{aligned}
\tag{2.18}
$$

where $^*\rho_l$ and $^*\rho_t$ are the corresponding spectral densities,

$$
{}^*\rho_{l,t}(q_0, q) = 2\mathrm{Im}\,{}^*\Delta_{l,t}(q_0 + i\eta, q). \tag{2.19}
$$

Note the subtraction performed in the spectral representation of $^*\Delta_l(\omega, q)$: this is necessary since $^*\Delta_l(\omega, q) \to -1/q^2$ as $|\omega| \to \infty$. When the above expressions are inserted in eq. (2.17), the sum over ω_m can be performed easily. One obtains then

$$
\Sigma(p) = -g^2 \int \frac{\mathrm{d}^3q}{(2\pi)^3} \int_{-\infty}^{+\infty} \frac{\mathrm{d}k^0}{2\pi} \int_{-\infty}^{+\infty} \frac{\mathrm{d}q^0}{2\pi} \rho_0(k)\gamma_\mu \not{k}\gamma_\nu {}^*\rho^{\mu\nu}(q) \frac{1 + N(q^0) - n(k^0)}{k^0 + q^0 - p^0}. \tag{2.20}
$$

The analytical continuation $p^0 \to \omega + i\eta$ can now be done, and the damping rate is calculated as $\gamma(p) = -\mathrm{Im}\,\Sigma_+(p, p)$. One gets:

$$
\begin{aligned}
\gamma(p) = {} & \frac{\pi g^2}{\omega} \int \frac{\mathrm{d}^3q}{(2\pi)^3} \int_{-\infty}^{+\infty} \frac{\mathrm{d}k^0}{2\pi} \int_{-\infty}^{+\infty} \frac{\mathrm{d}q^0}{2\pi} \delta(k^0 + q^0 - \omega) \left[1 + N(q^0) - n(k^0)\right] \\
& \rho_0(k) \left\{ 2\left[\omega k_0 - (\mathbf{p} \cdot \hat{\mathbf{q}})(\mathbf{k} \cdot \hat{\mathbf{q}})\right] {}^*\rho_t(q) + \left[\omega k_0 + (\mathbf{p} \cdot \mathbf{k})\right] {}^*\rho_l(q) \right\},
\end{aligned}
\tag{2.21}
$$

11

where $\omega = p$, $k^\mu = (k^0, \mathbf{k})$ and $\mathbf{k} = \mathbf{p} - \mathbf{q}$.

The spectral functions (2.19) of the dressed photon have the following structure:

$$^*\rho_s(q_0, q) = 2\pi\epsilon(q_0)\, z_s(q)\, \delta(q_0^2 - \omega_s^2(q)) + \beta_s(q_0, q)\theta(q^2 - q_0^2), \tag{2.22}$$

where $s = l$ or t, $z_s(q)$ is the residue of the time-like pole at $\omega_s(q)$, and

$$\begin{aligned}
\beta_l(q_0, q) &= 3\pi\omega_p^2 \frac{q_0}{q} |^*\Delta_l(q_0, q)|^2, \\
\beta_t(q_0, q) &= 3\pi\omega_p^2 \frac{q_0(q^2 - q_0^2)}{2q^3} |^*\Delta_t(q_0, q)|^2.
\end{aligned} \tag{2.23}$$

For $\omega \to p$, the energy conservation selects the positive value $k_0 = \epsilon_{p-q} \equiv |\mathbf{p} - \mathbf{q}|$ from the spectral density $\rho_0(k_0, k)$ of the internal fermion. Also, the kinematics restricts the photon momentum to be space-like ($|q_0| < q$). Finally, because of the infrared sensitivity of the damping rate, the whole contribution to Γ in the on-shell limit (and not only its divergent part) comes from *soft* photon momenta, $q \ll T$. Since, on the other hand, $p \sim T$, we can make the following kinematical approximations when evaluating eq. (2.21) (recall that $\omega = p$):

$$\begin{aligned}
\epsilon_{p-q} &\simeq p - \mathbf{p} \cdot \hat{\mathbf{q}} &= p - q\cos\theta, \\
\omega\epsilon_{p-q} - (\mathbf{p} \cdot \hat{\mathbf{q}})(\mathbf{k} \cdot \hat{\mathbf{q}}) &\simeq p^2(1 - \cos^2\theta), \\
\omega k_0 + (\mathbf{p} \cdot \mathbf{k}) &\simeq 2p^2, \\
1 + N(q^0) - n(\epsilon_{p-q}) &\simeq N(q^0) \simeq T/q^0.
\end{aligned} \tag{2.24}$$

With these simplifications, eq. (2.21) becomes

$$\begin{aligned}
\gamma(p) \simeq \pi g^2 T \int \frac{d^3q}{(2\pi)^3} \int_{-\infty}^{\infty} \frac{dq_0}{2\pi q_0}\, \delta(q_0 - q\cos\theta) \\
\left({}^*\rho_l(q) + (1 - \cos^2\theta)\, {}^*\rho_t(q)\right),
\end{aligned} \tag{2.25}$$

and it is independent of the external momentum. To be consistent with the approximations performed, we supply the above integral over q with an upper cut-off q^* satisfying $gT \ll q^* \ll T$. We shall verify later that, to the order of interest, the value of the integral is actually independent of q^*.

By using the δ-function to perform the angular integration in eq. (2.25), we obtain

$$\gamma \simeq \frac{g^2 T}{4\pi} \int_\mu^{q^*} dq\, q \int_{-q}^{q} \frac{dq_0}{2\pi q_0} \left\{ \beta_l(q_0, q) + \left(1 - \frac{q_0^2}{q^2}\right) \beta_t(q_0, q) \right\}. \tag{2.26}$$

In order to regularize the IR divergence, we have inserted a lower cut-off μ in the integral over q. Note that, because of the kinematics, the support of the energy integral is limited to $-q < q_0 < q$, so that only the off-shell pieces $\beta_{l,t}(q_0, q)$ of the photon spectral densities contribute to the damping rate. This is consistent with the physical interpretation of the damping rate presented in section 2.1. In fact, at this point, we can easily make contact between these two presentations. Namely, eq. (2.11) in section 2.1 is essentially the same as the above eq. (2.26), as can be seen by using eq. (2.23) for the spectral densities. Moreover, the IR singular piece of the damping rate (2.26) is given by eq. (2.15), as we verify now through a different computation, based on the sum-rules [18] displayed in Appendix A.

Using the behaviour of these sum-rules for large photon momenta $q \gg \omega_p$, as given in eq. (A.6), one can verify that γ is independent of the arbitrary intermediate scale q^*, to the order of interest (the contribution of the momenta $q > q^*$ is of relative order gT/q^*). Furthermore, the infrared behavior is dominated by that term of eq. (2.26) which involves the transverse spectral density divided by q_0. Specifically, for small momenta $q \ll \omega_p$ we can write

$$\int_{-q}^{q} \frac{dq_0}{2\pi q_0} \beta_t(q_0, q) = \frac{1}{q^2}\left(1 + \mathcal{O}(q^2/\omega_p^2)\right), \tag{2.27}$$

which diverges as $1/q^2$ in the zero momentum limit. All the other terms give finite contributions as $q \to 0$ (of relative order q^2/ω_p^2), and will be neglected here. By retaining only the leading term in eq. (2.27), we obtain the singular contribution to eq. (2.26):

$$\gamma_{sing} = \frac{g^2 T}{4\pi} \int_{\mu}^{\omega_p} dq \, \frac{1}{q} = \frac{g^2 T}{4\pi} \ln \frac{\omega_p}{\mu}. \tag{2.28}$$

The upper cut-off $\omega_p \sim gT$ accounts approximately for the terms which have been neglected when keeping only the $1/q^2$ contribution to the sum-rule (2.27) (recall that the full integrand in eq. (2.26) is indeed cut-off at $q \sim \omega_p$). As long as we are interested only in the coefficient of the logarithm, the precise value of this cut-off is unimportant. The scale ω_p however is uniquely determined by the physical process responsible for the existence of space like photons, i.e., the Landau damping. As we shall see later, this is the scale which fixes the long time behavior of the retarded propagator.

In terms of collisions, the logarithmic singularity of γ, eq. (2.28), arises from the exchange of very soft quasistatic ($q_0 \simeq 0$) magnetic photons, as already discussed in section 2.1. In the present computation, this may be seen also as follows: for very soft
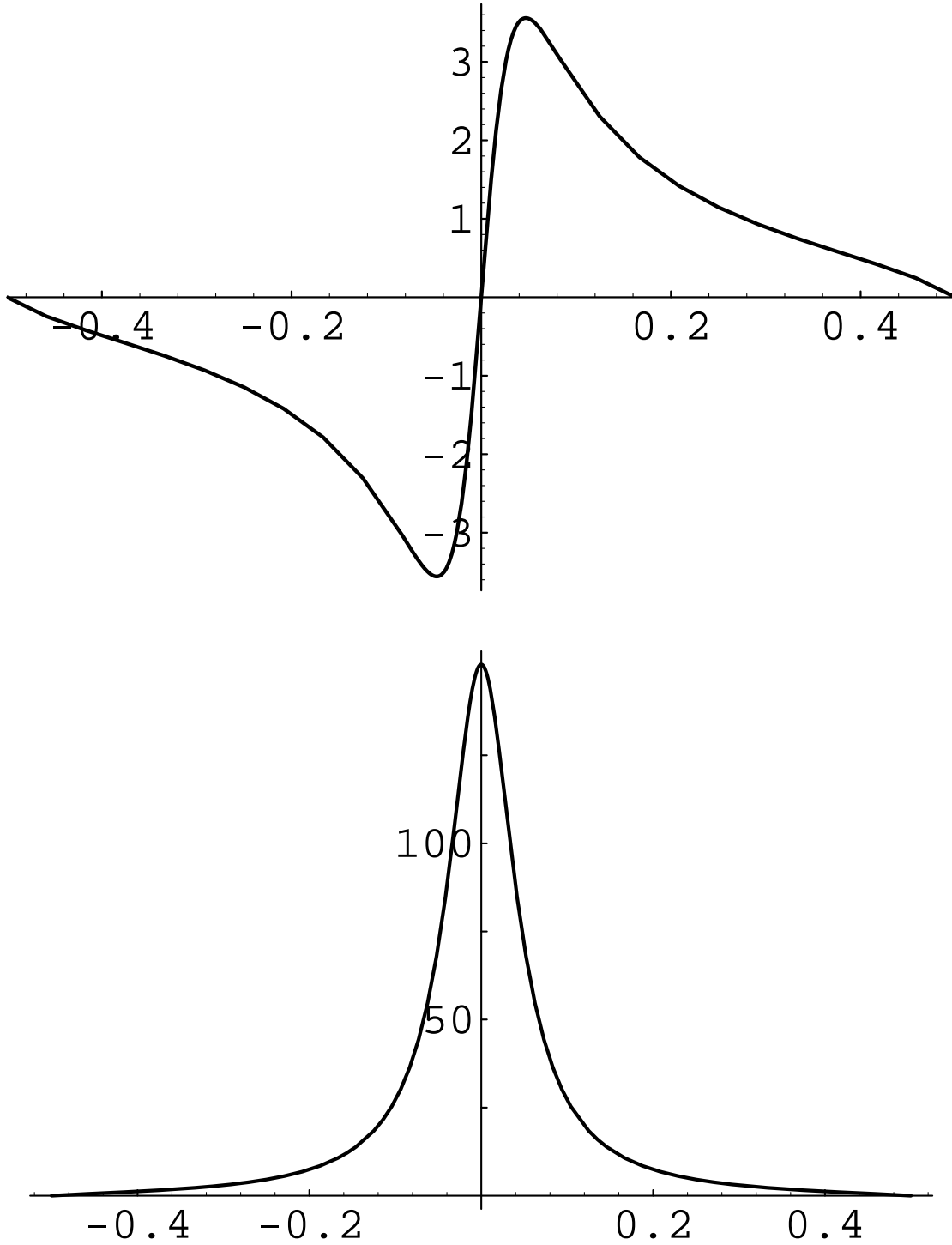
13

Figure 5: The functions $\beta_t(q_0, q)$ and $\beta_t(q_0, q)/q_0$ for $q = 0.5\,\omega_p$. All the quantities are made adimensional by multiplying them by appropriate powers of ω_p.

momenta $q \ll \omega_p$, the function $\beta_t(q_0, q)/q_0$ is strongly peaked at $q_0 = 0$ (see Fig. 5) and in the calculation of the integral (2.27) it can be replaced by the following approximate expression:

$$\frac{1}{q_0} \beta_t(q_0 \ll q) = \frac{3\pi}{2} \frac{\omega_p^2 q}{q^6 + (3\pi\omega_p^2 q_0/4)^2} \longrightarrow_{q\to 0} \frac{2\pi}{q^2} \delta(q_0). \qquad (2.29)$$

This is, of course, just a translation of the corresponding property (2.16) of the magnetic propagator. Still, this is suggestive as it shows that the density of states $\beta_t(q_0, q)N(q_0) \sim (T/q_0)\beta_t(q_0, q)$ which are available for the emission $(q_0 > 0)$ or the absorbtion $(q_0 < 0)$ of a virtual photon with momentum $\mathbf{q}$ and energy q_0 is *nonvanishing* in the zero-frequency limit $q_0 \to 0$, in spite of the fact that the spectral density $\beta_t(q_0, q)$ vanishes in the same limit. In fact, for very soft momenta $q \ll \omega_p$, the whole density of states is concentrated at $q_0 = 0$, as shown by eq. (2.29).

2.3 Static photon modes and non-perturbative aspects

Because of the delta function singularity $\delta(q_0)$ in eq. (2.29), the above discussion suggests that, in the imaginary time formalism, the whole IR singularity is concentrated in the static mode $q_0 = 0$. Let us verify this explicitly by showing that, indeed, the logarithm in eq. (2.28) arises entirely from the magnetic contribution of the *static* term $q_0 = i\omega_m = 0$ in the Matsubara sum of eq. (2.17) [16, 25]. Note that the analytic continuation of this term to real energy $(p_0 \to \omega + i\eta)$ is well-defined, since all its singularities lie on the real axis in the complex p_0 plane. (This is not so for the terms with $q_0 = i\omega_m \neq 0$, which individually have singularities off the real axis.)

The magnetostatic mode gives the following contribution to the one-loop self-energy:

$$
\begin{aligned}
\Sigma_s(\omega, \mathbf{p}) &= -g^2 T \int \frac{d^3q}{(2\pi)^3} \, \gamma^i \, S_0(\omega, \mathbf{p} - \mathbf{q}) \, \gamma^{j\,*} D^{ij}(0, \mathbf{q}) \\
&= g^2 T \int \frac{d^3q}{(2\pi)^3} \frac{\gamma^i(\omega\gamma^0 - (\mathbf{p} - \mathbf{q}) \cdot \boldsymbol{\gamma})\gamma^j}{(\omega + i\eta)^2 - (\mathbf{p} - \mathbf{q})^2} \frac{\delta^{ij} - \hat{q}^i\hat{q}^j}{\mathbf{q}^2} .
\end{aligned} \qquad (2.30)
$$

The momentum integral in eq. (2.30) shows a logarithmic *ultraviolet* divergence. In the full calculation, such a divergence would be cut-off by the contribution of the non static modes. (Recall the discussion after eq. (2.28).) When supplemented with an upper cut-off ω_p, eq. (2.30) yields the following contribution to the fermion damping rate (for $\omega \simeq p$):

$$\gamma_s \equiv -\frac{1}{4p} \operatorname{tr}\left(\not{p} \operatorname{Im} \Sigma_s(p)\right) \simeq g^2 T \int \frac{d^3q}{(2\pi)^3} \frac{1}{q^2} \operatorname{Im} \frac{-1}{\omega - p - q\cos\theta + i\eta}$$

15

$$\simeq \ \frac{g^2 T}{4\pi} \int_0^{\omega_p} \mathrm{d}q \int_{-1}^{1} \mathrm{d}\cos\theta \, \delta(\omega - p - q\cos\theta) \ = \ \alpha T \ln \frac{\omega_p}{|\omega - p|}, \qquad (2.31)$$

where the approximate equality means that only regular terms have been dropped. In the mass-shell limit $\omega \to p$, this reproduces the singular result of eq. (2.28). Note that the upper cut-off ω_p is the only trace of the screening effects in the above calculation: indeed, the magnetostatic propagator is the same as at the tree-level, namely ${}^*\Delta(0, q) = 1/q^2$.

The divergence of γ at the (resummed) one-loop level invites a closer examination of the higher order corrections. The two-loop self-energy is briefly discussed in Appendix C, where we show that the leading infrared divergence arises, again from terms where both the internal photons are static and magnetic. This result is readily generalized to all orders: the most singular contributions to the on-shell fermion self-energy are confined to the magnetostatic sector. When computing these contributions, all the loop integrals run over the three momenta $\mathbf{q}$ of the static internal photons, so that the infrared singularities are effectively those of a *three-dimensional* theory. Consider then a generic n-loop self-energy diagram with only magnetostatic modes: Its discontinuity, when evaluated on the tree-level mass-shell $\omega = p$, has power-like IR divergences, possibly combined with logarithmic ones. Power counting shows that the leading divergences are of relative order $(g^2 T/\mu)^{n-1}$, where μ is an IR cut-off. Such strong IR divergences are analogous to those identified in the analysis of the corrections to the screening mass in [44], and their presence signals a breakdown of perturbation theory.

To get further insight, it is useful to consider the explicit two-loop calculation from Appendix C: the on-shell self-energy $\Sigma^{(2)}(p, \mathbf{p})$ shows a linear plus logarithmic divergence. (There are also subleading, purely logarithmic, divergences, but these are left out in a leading-order calculation.) Specifically, eq. (C.5) yields

$$\Sigma_+^{(2)}(p, p) \equiv \frac{1}{2} \mathrm{tr}\Big(h_\pm(\hat{\mathbf{p}})\Sigma^{(2)}(p, p)\Big) \ \simeq \ i\frac{2}{\pi} \frac{(\alpha T)^2}{\mu} \ln \frac{\omega_p}{\mu} \ \sim \ \frac{\alpha T}{\mu} \Sigma_+^{(1)}(p, p), \qquad (2.32)$$

where $\Sigma_+^{(1)}(p, p) = -i\alpha T \ln(\omega_p/\mu)$ is the on-shell limit of the one-loop self-energy in eq. (2.31). Now, in order to compute the two-loop contribution to the damping rate, one has to expand the dispersion equation $\omega = p + \Sigma_+(\omega, p)$ up to the order of interest. This yields the 2-loop mass-shell correction in the form

$$\delta\omega^{(2)}(p) = [z^{(1)}(p) - 1]\Sigma_+^{(1)}(p, p) + \Sigma_+^{(2)}(p, p) + \mathcal{O}(3 \text{ loops}), \qquad (2.33)$$

16

where

$$z^{(1)}(p) - 1 = \frac{\partial \Sigma_+^{(1)}}{\partial \omega}\bigg|_{\omega=p} \simeq \frac{2}{\pi} \frac{\alpha T}{\mu} \qquad (2.34)$$

is the one-loop residue, whose leading IR-divergent part has been computed in the Appendix. By combining eqs. (2.32) and (2.33)–(2.34), we note that the leading, power-like, divergences cancel between the two-loop self-energy and the one-loop residue, so that the two-loop correction to γ is only logarithmically divergent, as at the one loop level.

A simple argument, based on a gauge-invariant approximation to the full Dyson-Schwinger equation which is detailed in Appendix C, suggests that this is a general feature: *if we assume the fermion propagator to have a simple pole at the mass-shell*, then the damping rate remains *logarithmically* divergent to *all* orders. That is, the power-like divergences which occur in $\Sigma(\omega = p)$ appear to cancel against similar divergences in the residue. (A similar all-order cancellation has been argued in three-dimensional QED at zero temperature[45].) However, the persistence of the logarithmic divergence in all orders of perturbation theory suggests that the analytic structure of the propagator is more complicated than a simple pole.

To conclude this section, let us emphasize that when we compute the imaginary part of multi-loop diagrams with only static internal photons, we are actually considering the effects of multiple collisions involving the exchange of quasistatic magnetic photons with the plasma particles. The fact that these processes (or, more accurately, their most IR singular contributions to the interaction rate) can be effectively taken into account by the "dimensional reduction" to the magnetostatic photon modes is a consequence of the specific infrared behaviour of the resummed magnetic propagator, as expressed by eq. (2.16).

3   The Bloch-Nordsieck model at finite temperature

Previously, we have shown that the leading infrared divergences in the perturbative computation of the fermion self-energy are those of an effective three-dimensional theory involving only static magnetic photons. We shall take advantage of this in order to get an explicit expression for the fermion propagator. However, before restricting ourselves to the static photon modes, we shall first develop a more general approach which is essentially a finite-temperature extension of the Bloch-Nordsieck approximation[32, 33].
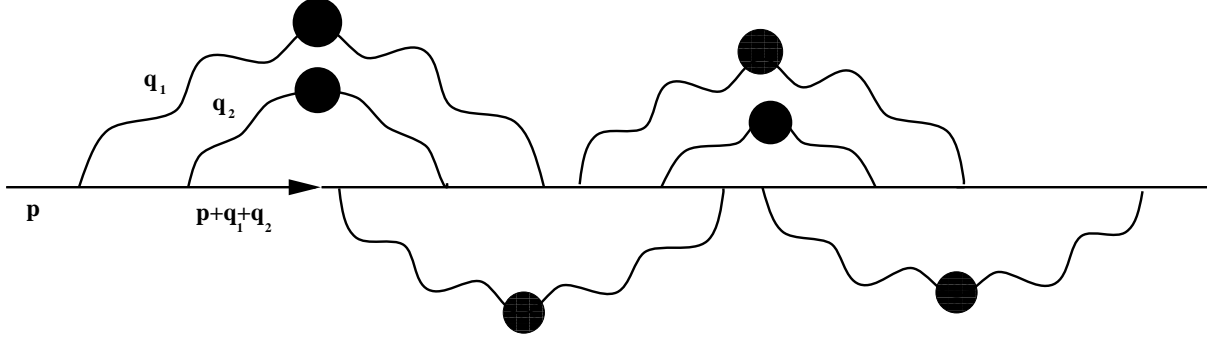
Figure 6: A generic n-loop diagram (here, $n = 6$) for the self-energy in quenched QED.

3.1 Perturbation theory with soft photons

We start by deriving a set of simplified Feynman rules which allows one to compute the most IR singular contributions to the damping rate from higher loop self-energy diagrams. The leading infrared divergences arise from diagrams where *all* the internal photon lines are soft, and therefore dressed by the screening corrections. No further resummation of the photon lines is necessary beyond the hard termal loop approximation: in abelian gauge theories, all the higher order corrections to the photon polarisation tensor remain perturbative, and do not modify the qualitative IR behavior of the HTL-resummed propagator (denoted as $^*D_{\mu\nu}(q)$).

Thus, when expressed in terms of the resummed photon propagator, the relevant self-energy diagrams contain no fermion loops: the internal photon lines are all attached on the incoming fermion line. A typical n-loop diagram is shown in Fig. 6. There are as many loops as photon propagators, and we can chose all the independent loop momenta to be the momenta q_r of the soft photon lines (here $r = 1, ..., n$ for an n-loop graph). All such diagrams are composed from the three following structural units:

(i) the effective photon propagator $^*D_{\mu\nu}(q)$;

(ii) the fermion propagator $S_0(p + q)$, where p is the hard external momentum, and q is a linear combination of the soft loop momenta;

(iii) the photon-fermion vertex γ^μ.

In the kinematical regime of interest, both the fermion propagator and the vertex function can be further simplified, along the lines explained in Section 2.2. After performing the Matsubara sums over the internal bosonic frequencies, and the analytic continuation to real external energy, the internal fermion lines are represented by spectral densities like

(see, e.g., eq. (2.20))

$$\rho_{\mathrm{f}}(k^0, \mathbf{p} - \mathbf{q}) = \left(k^0\gamma^0 - (\mathbf{p} - \mathbf{q}) \cdot \boldsymbol{\gamma}\right)\frac{\pi}{\epsilon_{p-q}}\left(\delta(k^0 - \epsilon_{p-q}) - \delta(k^0 + \epsilon_{p-q})\right), \tag{3.1}$$

which multiply energy denominators of the form $1/(\omega - k^0 - q^0)$. Since $q \ll p$, we can use $\epsilon_{p-q} \simeq \epsilon_p - \mathbf{v} \cdot \mathbf{q} = p - q\cos\theta$ (where $\mathbf{v} = \partial\epsilon_p/\partial\mathbf{p} = \hat{\mathbf{p}}$) to replace eq. (3.1) with

$$\acute{\rho}_{\mathrm{f}}(k^0, \mathbf{p} - \mathbf{q}) \equiv (\gamma^0 - \hat{\mathbf{p}} \cdot \boldsymbol{\gamma})\pi\delta(k^0 - \mathbf{v} \cdot (\mathbf{p} - \mathbf{q})) = h_+(\hat{\mathbf{p}})\acute{\rho}_0(k^0, \mathbf{p} - \mathbf{q}), \tag{3.2}$$

where the reduced spectral density

$$\acute{\rho}_0(\omega, \mathbf{p}) \equiv 2\pi\delta(\omega - \mathbf{v} \cdot \mathbf{p}) \tag{3.3}$$

involves only the positive-energy fermion state. The contribution of the negative-energy fermion state, initially present in eq. (3.1), is suppressed by the corresponding large energy denominator.

One sees on eq. (3.2) that neither the spin structure, nor the negative-energy fermion intermediate states, play an important role. In fact, the residual spin structure of eq. (3.2), i.e. the spin matrix $h_+(\hat{\mathbf{p}})$, does not involve the loop momenta anymore, and can be absorbed into a redefinition of the vertex function. To see this, recall that, for a positive energy hard fermion, the relevant self-energy is $\Sigma_+ = \mathrm{tr}\,(h_+(\hat{\mathbf{p}})\Sigma)/2$. In the present kinematical regime, the spin structure of a typical n-loop contribution to Σ_+ factorizes into the trace

$$I^{\mu_1\mu_2\,\cdots\,\mu_{2n}} = \frac{1}{2}\,\mathrm{tr}\,\left\{h_+(\hat{\mathbf{p}})\gamma^{\mu_1}h_+(\hat{\mathbf{p}})\gamma^{\mu_2}\ldots h_+(\hat{\mathbf{p}})\gamma^{\mu_{2n}}\right\}. \tag{3.4}$$

By using the identities (with $v^\mu = (1, \mathbf{v})$)

$$\begin{aligned} h_+(\hat{\mathbf{p}})\gamma^\mu h_+(\hat{\mathbf{p}}) &= v^\mu h_+(\hat{\mathbf{p}}), \\ \mathrm{tr}\left(h_+(\hat{\mathbf{p}})\gamma^\mu\right) &= 2v^\mu, \end{aligned} \tag{3.5}$$

one readily derives

$$I^{\mu_1\mu_2\,\cdots\,\mu_{2n}} = v^{\mu_1}\,v^{\mu_2}\ldots v^{\mu_{2n}}\,. \tag{3.6}$$

The same result would have been obtained by using the reduced spectral density (3.3) instead of (3.2), together with the effective vertex $\Gamma^\mu = v^\mu$.

To conclude, the corrections to the self-energy Σ_+ which derive from the fermion interactions with soft photons can be obtained from the Feynman graphs of quenched

QED, by evaluating the latter with the following effective Feynman rules:

(i) the photon propagator $^*D_{\mu\nu}(q)$;

(ii) the fermion (analytic) propagator

$$G_0(p-q) = \int_{-\infty}^{+\infty} \frac{dk^0}{2\pi} \frac{\acute{\rho}_0(k^0, \mathbf{p}-\mathbf{q})}{k^0 - (p^0 - q^0)} = \frac{-1}{(p^0 - q^0) - \mathbf{v} \cdot (\mathbf{p}-\mathbf{q})}; \qquad (3.7)$$

(iii) the photon-fermion vertex $\Gamma^\mu = v^\mu$.

Any reference to the spin structure, and also to the antiparticles, has disappeared.

We note that, when used in relation to the one-loop self-energy in Fig. 4, the above Feynman rules yield directly the expression (2.26) for the damping rate (that is, the *whole* contribution of order g^2T, and not only its divergent piece). For higher loop diagrams however, we do not expect all the subleading divergences to be correctly reproduced since, for instance, contributions coming from mixed diagrams, where some photons are hard and the other ones are soft, have been ignored.

The simplified structure which is put forward here is familiar from most treatements of the IR divergences at zero temperature (see, e.g., [46] and references therein). It can be most economically exploited within the Bloch-Nordsieck model[32] (see also [33]), which, for the vaccuum theory, is exactly soluble. In order to search for a non-perturbative solution at finite temperature, we follow Ref. [33] and reformulate this model in the language of path integrals.

3.2   The Bloch-Nordsieck model in functional form

In the Matsubara formalism, the exact fermion propagator at finite temperature can be obtained as

$$S_E(x, y) = Z^{-1} \int [dA] \, S_E(x, y|A) \exp \left\{ -\mathrm{Tr} \ln S_E(x, y|A) - \frac{1}{2} \left(A, D_0^{-1}A \right) \right\} \qquad (3.8)$$

where $S_E(x, y|A)$ is the (imaginary-time) fermion propagator in the presence of a background gauge field:

$$-i\slashed{D}_x S_E(x, y|A) = \delta_E(x - y), \qquad (3.9)$$

and $D_\mu = \partial_\mu + igA_\mu$. In these equations, the time variables are purely imaginary (e.g., $x_0 = -i\tau_x$ and $y_0 = -i\tau_y$, with $0 \le \tau_x, \tau_y \le \beta$ and $\delta_E(x - y) = \delta(\tau_x - \tau_y)\delta(\mathbf{x} - \mathbf{y})$),

and the gauge fields are periodic in time, $A_\mu(\tau = 0) = A_\mu(\tau = \beta)$. The tree-level photon action has been written as

$$\left(A, D_0^{-1} A\right) \; = \; T \sum_m \int \frac{\mathrm{d}^3 q}{(2\pi)^3} \, A^\mu(i\omega_m, \mathbf{q}) \, D_{0\,\mu\nu}^{-1}(i\omega_m, \mathbf{q}) A^\nu(-i\omega_m, -\mathbf{q}), \tag{3.10}$$

where $\omega_m = 2\pi m T$ with integer m, and $D_{0\,\mu\nu}$ is the free photon propagator in an arbitrary gauge.

The fermion propagators $S_E(x - y)$ and $S_E(x, y|A)$ are antiperiodic. For instance,

$$S_E(\tau_x = 0, \tau_y|A) = -S_E(\tau_x = \beta, \tau_y|A), \tag{3.11}$$

and similarly for τ_y. The functional determinant $\exp\{-\mathrm{Tr} \ln S_E(x, y|A)\}$ describes the plasma polarization. Diagrammatically, this terms generates internal fermion loops. As already discussed, the only polarization effects which need to be considered are those contained in the photon HTL, which we denote here as $\delta\Pi_{\mu\nu}$:

$$\mathrm{Tr} \ln S_E(x, y|A) \simeq \frac{1}{2} \left(A, \, \delta\Pi \, A\right). \tag{3.12}$$

Furthermore, the simplifications discussed in the previous subsection are easily implemented by replacing the exact propagator $S_E(x, y|A)$ in eq. (3.8) with the Bloch-Nordsieck propagator $G_E(x, y|A)$, solution of the equation

$$- i \left(v \cdot D_x\right) G_E(x, y|A) \; = \; \delta_E(x - y), \tag{3.13}$$

with antiperiodic boundary conditions. (Formally, this equation is obtained by replacing the Dirac matrices γ^μ by the particle velocity v^μ in the full equation (3.9)). With the above simplifications, the general equation (3.8) reduces to

$$S_E(x, y) = Z^{-1} \int [\mathrm{d}A] \, G_E(x, y|A) \exp\left\{-\frac{1}{2} \left(A, \, {}^*D^{-1}A\right)\right\}, \tag{3.14}$$

with ${}^*D_{\mu\nu}^{-1} = D_{0\,\mu\nu}^{-1} + \delta\Pi_{\mu\nu}$. It is easy to verify that, when considered in perturbation theory, eqs. (3.13) and (3.14) generate the simplified Feynman rules alluded to at the end of the previous subsection.

3.3 The Bloch-Nordsieck propagator in imaginary-time

In real-time, the equation for $G(x, y|A)$ reads

$$- i \left(v \cdot D_x\right) G(x, y|A) \; = \; \delta^{(4)}(x - y), \tag{3.15}$$

21

and can be solved *exactly*. For retarded boundary conditions, $G(x, y|A) = 0$ for $x_0 < y_0$, the solution reads

$$
\begin{aligned}
G_R(x, y|A) &= i\,\theta(x^0 - y^0)\,\delta^{(3)}\left(\mathbf{x} - \mathbf{y} - \mathbf{v}(x^0 - y^0)\right) U(x, y) \\
&= i \int_0^\infty dt\, \delta^{(4)}(x - y - vt)\, U(x, x - vt).
\end{aligned}
\tag{3.16}
$$

Here, $U(x, y)$ is the parallel transporter along the straight line trajectory of velocity $\mathbf{v}$ joining x and y ($y = x - vt$):

$$
U(x, x - vt) = \exp\left\{ -ig \int_0^t ds\, v \cdot A(x - v(t - s)) \right\}.
\tag{3.17}
$$

In order to verify that (3.16) is indeed a solution of eq. (3.15), one may use the fact that the function $U(x, x - vt)$ satisfies the following equation,

$$
-\frac{\partial}{\partial t} U(x, x - vt) = (v \cdot D_x)\, U(x, x - vt),
\tag{3.18}
$$

with the boundary condition $U = 1$ for $t = 0$.

In imaginary-time, the resolution of eq. (3.13) is complicated by the antiperiodic boundary conditions to be imposed on G_E:

$$
G_E(\tau_x = 0, \tau_y|A) = -G_E(\tau_x = \beta, \tau_y|A),
\tag{3.19}
$$

and similarly for τ_y. The free equation ($A = 0$) can be easily solved in momentum space:

$$
G_E(i\omega_n, \mathbf{p}) = \frac{1}{\mathbf{v} \cdot \mathbf{p} - i\omega_n},
\tag{3.20}
$$

where $\omega_n = (2n + 1)\pi T$. This is in agreement with eq. (3.7). In the imaginary time representation,

$$
G_E(\tau, \mathbf{p}) = \sum_{\omega_n} e^{-i\omega_n \tau}\, G_E(i\omega_n, \mathbf{p}) = e^{-\mathbf{v} \cdot \mathbf{p}\tau} \left[\theta(\tau)(1 - n(\mathbf{v} \cdot \mathbf{p})) - \theta(-\tau)n(\mathbf{v} \cdot \mathbf{p}) \right],
\tag{3.21}
$$

where $n(\omega) = 1/\left(\exp(\beta\omega) + 1 \right)$ is the Fermi-Dirac statistical factor.

Consider now the interacting problem, with $A \neq 0$. As a guidance in searching a solution to eq. (3.13) with antiperiodic boundary conditions, we use the solution (3.16) to the real-time problem, which we write in the form (with $p^\mu = (\omega, \mathbf{p})$ and $v \cdot p = \omega - bf v \cdot p$)

$$
\begin{aligned}
G_R(x, y|A) &= \int \frac{d^4p}{(2\pi)^4}\, e^{-ip \cdot (x - y)} G_R(x, p|A) \\
G_R(x, p|A) &= i \int_0^\infty du\, e^{it(v \cdot p) - \eta t} U(x, x - vt),
\end{aligned}
\tag{3.22}
$$

where the x-dependence of the function $G_R(x, p|A)$ comes from the corresponding dependence of the background field.

By analogy, we look for the solution $G_E(x, y|A)$ to the imaginary-time BN equation in the following form[§]

$$
\begin{aligned}
G_E(x, y|A) &= \int \{dp\}\, e^{-ip \cdot (x-y)} G_E(x, p|A) \\
G_E(x, p|A) &= -\int_0^\beta du\, e^{-u(v \cdot p)} V(x, \mathbf{v} \cdot \mathbf{p}; u),
\end{aligned}
\tag{3.23}
$$

where the unknown function $V(x, \mathbf{v} \cdot \mathbf{p}; u)$ satisfies

$$
\begin{aligned}
-\frac{\partial}{\partial u} V &= i(v \cdot D_x) V, \\
V(\tau_x = 0; u) &= V(\tau_x = \beta; u), \\
V(x, \mathbf{v} \cdot \mathbf{p}; u = 0) &+ e^{\beta(\mathbf{v} \cdot \mathbf{p})} V(x, \mathbf{v} \cdot \mathbf{p}; u = \beta) = 1.
\end{aligned}
\tag{3.24}
$$

As in the real-time case, the x-dependence of $G_E(x, p|A)$ arises entirely from its interactions with the (periodic) gauge field. If $A = 0$, we recover the free propagator (3.20) by replacing $V(x, \mathbf{v} \cdot \mathbf{p}; u)$ with $n(\mathbf{v} \cdot \mathbf{p})$, which satisfies indeed the last equation (3.24) because of the identity

$$
n(\epsilon) + e^{\beta \epsilon} n(\epsilon) = 1.
\tag{3.25}
$$

Eq. (3.24), with the indicated boundary conditions, can be solved as a series in powers of gA_μ, that is, as a perturbative expansion:

$$
\begin{aligned}
V(x, \mathbf{v} \cdot \mathbf{p}; u) &= n(\mathbf{v} \cdot \mathbf{p}) + g \int [dq]\, e^{-iq \cdot x} \frac{v \cdot A(q)}{v \cdot q} \left[n(\mathbf{v} \cdot \mathbf{p}) - n(\mathbf{v} \cdot (\mathbf{p} + \mathbf{q})) e^{-u(v \cdot q)} \right] \\
&+ \frac{g^2}{2} \int [dq_1][dq_2]\, e^{-i(q_1 + q_2) \cdot x} \frac{v \cdot A(q_1)}{v \cdot q_1} \frac{v \cdot A(q_2)}{v \cdot q_2} \\
&\quad \left[n(\mathbf{v} \cdot \mathbf{p}) - n(\mathbf{v} \cdot (\mathbf{p} + \mathbf{q_1})) e^{-u(v \cdot q_1)} - n(\mathbf{v} \cdot (\mathbf{p} + \mathbf{q_2})) e^{-u(v \cdot q_2)} \right. \\
&\quad \left. + n(\mathbf{v} \cdot (\mathbf{p} + \mathbf{q_1} + \mathbf{q_2})) e^{-u\, v \cdot (q_1 + q_2)} \right] + \dots.
\end{aligned}
\tag{3.26}
$$

It can be verified, using in particular the identity (3.25), that the series (3.26) satisfies indeed eqs. (3.24).

[§]To simplify notations, the measure in the momentum integrals will be denoted below by the following condensed notation:

$$
\int [dq] \equiv T \sum_{q_0, even} \int \frac{d^3 q}{(2\pi)^3}, \qquad \int \{dp\} \equiv T \sum_{p_0, odd} \int \frac{d^3 p}{(2\pi)^3}.
$$

As already noted, the quantity $V(x, \mathbf{v} \cdot \mathbf{p}; u)$ is the imaginary-time analogue of the real-time parallel transporter $U(x, x - vt)$, eq. (3.17). This is also manifest from the analogy between eq. (3.18) for $U(x, x - vt)$ and eq. (3.24) for $V(x, \mathbf{v} \cdot \mathbf{p}; u)$. By solving eq. (3.18) in perturbation theory, one generates a series analogous to (3.26), where, however, the thermal factors are absent. The correspondance between the two series can be easily worked out term by term. For instance,

$$\left[n(\mathbf{v} \cdot \mathbf{p}) - n(\mathbf{v} \cdot (\mathbf{p} + \mathbf{q})) e^{-u(v \cdot q)} \right] \rightarrow \left(1 - e^{it(v \cdot q)} \right),$$

and so on. In the real-time series, factorisations occur, which bring in simplifications. For example, in second order,

$$\left(1 - e^{it(v \cdot q_1)} - e^{it(v \cdot q_2)} + e^{it(v \cdot q_1 + v \cdot q_2)} \right) = \left(1 - e^{it(v \cdot q_1)} \right) \left(1 - e^{it(v \cdot q_2)} \right).$$

Because of such factorisations, the real-time series corresponding to eq. (3.26) can be resummed into an exponential, leading to the expression (3.17). In the imaginary-time, the presence of the thermal factors prevents such a simple exponentiation.

By inserting $G_E(x, y | A)$, eqs. (3.23) and (3.26), into eq. (3.14), we can perform the gaussian functional integral over the photon fields term by term. This yields:

$$\begin{aligned} S_E(x - y) &= \int \{\mathrm{d}p\} \, e^{-ip \cdot (x-y)} S_E(p) \\ S_E(p) &= -\int_0^\beta \mathrm{d}u \, e^{-u(v \cdot p)} \, \tilde{V}(\mathbf{v} \cdot \mathbf{p}; u), \end{aligned} \qquad (3.27)$$

where $\tilde{V}(\mathbf{v} \cdot \mathbf{p}; u)$ is the functional average of $V(x, \mathbf{v} \cdot \mathbf{p}; u)$, eq. (3.26),

$$\begin{aligned} \tilde{V}(\mathbf{v} \cdot \mathbf{p}; u) = \ & n(\mathbf{v} \cdot \mathbf{p}) + \sum_{n \geq 1} (-1)^n \frac{g^{2n}}{n!} \int [\mathrm{d}q_1 \mathrm{d}q_2 \dots \mathrm{d}q_n] \frac{\tilde{D}(q_1) \tilde{D}(q_2) \dots \tilde{D}(q_n)}{(v \cdot q_1)^2 (v \cdot q_2)^2 \dots (v \cdot q_n)^2} \\ & \left[n(\mathbf{v} \cdot \mathbf{p}) - n(\mathbf{v} \cdot (\mathbf{p} + \mathbf{q_1})) e^{-u(v \cdot q_1)} - n(\mathbf{v} \cdot (\mathbf{p} + \mathbf{q_2})) e^{-u(v \cdot q_2)} + \right. \\ & \left. \dots + (-1)^n n(\mathbf{v} \cdot (\mathbf{p} + \mathbf{q_1} + \mathbf{q_2} + \dots + \mathbf{q_n})) e^{-u v \cdot (q_1 + q_2 + \dots + q_n)} \right], \quad (3.28) \end{aligned}$$

and

$$\tilde{D}(q) = v^{\mu *} D_{\mu\nu}(i\omega_m, \mathbf{q}) v^\nu . \qquad (3.29)$$

Eqs. (3.27)–(3.28) express the Matsubara fermion propagator in the Bloch-Nordsieck model as a formal series in powers of g^2.

3.4   The retarded propagator

To study the mass-shell behavior of the fermion propagator, we need the *retarded* propagator, rather than the Matsubara one. These two propagators are related by analytic continuation in either the complex energy, or the complex time, plane. Here it is more convenient to proceed in the time representation. To this aim, we recall that the retarded propagator $S_R(t, \mathbf{p})$ can be obtained as

$$S_R(t, \mathbf{p}) \;=\; i\theta(t)\big(S^>(t, \mathbf{p}) + S^<(t, \mathbf{p})\big), \tag{3.30}$$

where the functions $S^>$ and $S^<$ are the analytic components of the time-ordered propagator[14, 13]. These can be obtained from the Matsubara propagator:

$$S_E(\tau, \mathbf{p}) \;=\; \theta(\tau)S^>(\tau, \mathbf{p}) - \theta(-\tau)S^<(\tau, \mathbf{p}). \tag{3.31}$$

In order to get the Matsubara propagator we have to evaluate first the sum over $p_0 = i\omega_n$ in eq. (3.27). Since $\tilde{V}(\mathbf{v} \cdot \mathbf{p}; u)$ is independent of p_0, this may be done trivially, by using

$$T \sum_{n,\,odd} e^{-i\omega_n(\tau+u)} = \delta(\tau + u) - \delta(\tau + u - \beta). \tag{3.32}$$

Then, for $-\beta \leq \tau \leq 0$, we obtain

$$
\begin{aligned}
S^<(\tau, \mathbf{x}) &\;=\; \int \frac{d^3p}{(2\pi)^3}\, e^{i\mathbf{p}\cdot\mathbf{x}}\, S^<(\tau, \mathbf{p}), \\
S^<(\tau, \mathbf{p}) &\;=\; e^{-\tau(\mathbf{V}\,\cdot\,\mathbf{P})}\tilde{V}(\mathbf{v} \cdot \mathbf{p}; u = -\tau),
\end{aligned}
\tag{3.33}
$$

and similarly, for $0 \leq \tau \leq \beta$,

$$S^>(\tau, \mathbf{p}) \;=\; e^{(\beta-\tau)(\mathbf{V}\,\cdot\,\mathbf{P})}\tilde{V}(\mathbf{v} \cdot \mathbf{p}; u = \beta - \tau). \tag{3.34}$$

In particular, the last eq. (3.24) implies

$$S^>(0, \mathbf{p}) \;+\; S^<(0, \mathbf{p}) \;=\; 1. \tag{3.35}$$

If the functions $S^<(\tau)$ and $S^>(\tau)$ are known explicitly, then they can be analytically extended in the complex time plane by simply replacing $\tau \to it$, with complex t. The functions $S^<(t)$ and $S^>(t)$ thus obtained are well defined for any t satisfying $0 \leq \operatorname{Im} t \leq \beta$, in the case of $S^<(t)$, and $-\beta \leq \operatorname{Im} t \leq 0$, for $S^>(t)$. For the problem at hand, these analytic

25

properties can be verified on eq. (3.28): they arise from the fact that the thermal factors render the momentum integrals like

$$\int \frac{\mathrm{d}^3 q}{(2\pi)^3}\, n(\mathbf{v} \cdot (\mathbf{p} + \mathbf{q}))\, \mathrm{e}^{u(\mathbf{v} \cdot \mathbf{q})}$$

convergent for any $0 < u < \beta$. We see that the statistical factors are essential to ensure the correct analytical properties; but, at the same time, they prevent the exponentiation in eq. (3.28).

According to eqs. (3.30), (3.33) and (3.34), the retarded propagator is given by

$$S_R(t, \mathbf{p}) = i\theta(t)\mathrm{e}^{-it(\mathbf{V} \cdot \mathbf{P})}\Big(\mathrm{e}^{\beta(\mathbf{V} \cdot \mathbf{P})}\tilde{V}(\mathbf{v} \cdot \mathbf{p}; u = \beta - it) + \tilde{V}(\mathbf{v} \cdot \mathbf{p}; u = -it)\Big). \quad (3.36)$$

The analytic continuation of the function $\tilde{V}(\mathbf{v} \cdot \mathbf{p}; u)$ to real time is permitted only *after* performing the Matsubara sums over the bosonic frequencies $q^0 = i\omega_m$ in all the terms of the infinite series (3.28). Fortunately, we may avoid doing this if we restrict ourselves to resumming the *leading* infrared divergences. This is further explained in the next subsection.

3.5   Dimensional reduction

In view of the discussion in section 2.3, the most IR singular terms of the perturbative expansion are concentrated in the static photon modes. Considering only the contribution of the static modes $q_0 = i\omega_m = 0$ to eq. (3.28) is equivalent to solving the Bloch-Nordsieck equation (3.13) in the presence of a *static* background field $A_\mu(\mathbf{x})$:

$$A^\mu(\mathbf{x}) = T \int \frac{\mathrm{d}^3 q}{(2\pi)^3}\, \mathrm{e}^{i\mathbf{q}\cdot\mathbf{x}} A_\mu(\omega_m = 0, \mathbf{q}) = T \int_0^\beta \mathrm{d}\tau\, A_\mu(\tau, \mathbf{x}). \quad (3.37)$$

With only static photon modes, the analytic continuation of eq. (3.28) to real time is trivial, and the sum in eq. (3.36) can be performed explicitly, term by term. As we show now, the thermal occupation factors *compensate in this sum*, and the resulting series for $S_R(t, \mathbf{p})$ can be resummed as an exponential. To be specific, consider the term of order g^2 in the expansion (3.28). To $\tilde{V}(\mathbf{v} \cdot \mathbf{p}; u = -it)$, this terms contributes ($\tilde{D}(\mathbf{q}) \equiv \tilde{D}(0, \mathbf{q})$)

$$-g^2 T \int \frac{\mathrm{d}^3 q}{(2\pi)^3} \frac{\tilde{D}(\mathbf{q})}{(\mathbf{v} \cdot \mathbf{q})^2} \Big[n(\mathbf{v} \cdot \mathbf{p}) - n(\mathbf{v} \cdot (\mathbf{p} + \mathbf{q}))\, \mathrm{e}^{-it(\mathbf{V} \cdot \mathbf{q})}\Big], \quad (3.38)$$

while to $\mathrm{e}^{\beta(\mathbf{V} \cdot \mathbf{P})}\tilde{V}(\mathbf{v} \cdot \mathbf{p}; u = \beta - it)$ it contributes

$$-g^2 T \int \frac{\mathrm{d}^3 q}{(2\pi)^3} \frac{\tilde{D}(\mathbf{q})}{(\mathbf{v} \cdot \mathbf{q})^2}\, \mathrm{e}^{\beta(\mathbf{V} \cdot \mathbf{P})} \Big[n(\mathbf{v} \cdot \mathbf{p}) - n(\mathbf{v} \cdot (\mathbf{p} + \mathbf{q}))\, \mathrm{e}^{\beta(\mathbf{V} \cdot \mathbf{q})}\mathrm{e}^{-it(\mathbf{V} \cdot \mathbf{q})}\Big]. \quad (3.39)$$

In the sum of these two expressions, the thermal factors disappear because of the identity (3.25), leaving

$$-g^2 T \int \frac{\mathrm{d}^3 q}{(2\pi)^3} \frac{\tilde{D}(\mathbf{q})}{(\mathbf{v} \cdot \mathbf{q})^2} \left(1 - \mathrm{e}^{-it(\mathbf{v} \cdot \mathbf{q})}\right). \tag{3.40}$$

By analyzing similar compensations for the higher order terms, we eventually recognize the power expansion of an exponential:

$$S_R(t, \mathbf{p}) = i\theta(t)\mathrm{e}^{-it(\mathbf{v} \cdot \mathbf{p})}\Delta(t), \tag{3.41}$$

with

$$\Delta(t) \equiv \exp\left\{-g^2 T \int \frac{\mathrm{d}^3 q}{(2\pi)^3} \frac{\tilde{D}(\mathbf{q})}{(\mathbf{v} \cdot \mathbf{q})^2} \left(1 - \cos t(\mathbf{v} \cdot \mathbf{q})\right)\right\}. \tag{3.42}$$

The zero-frequency photon propagator reads

$$\tilde{D}(\mathbf{q}) \equiv v^{\mu *} D_{\mu\nu}(\omega_m = 0, \mathbf{q}) v^\nu = -\frac{1}{q^2 + m_D^2} + \frac{1}{q^2}\left(1 - \frac{(\mathbf{v} \cdot \mathbf{q})^2}{q^2}\right) + \lambda \frac{(\mathbf{v} \cdot \mathbf{q})^2}{q^4}, \tag{3.43}$$

in an arbitrary gauge of the Coulomb or the covariant type ($\lambda = 0$ corresponds to both the Landau and the strict Coulomb gauges). The three terms in eq. (3.43) corresponds respectively to the electric, magnetic and gauge sector. In eq. (3.42), we have replaced the complex exponential by a cosine function, by taking into account the parity of the integrand.

The q-integral in eq. (3.42) presents a spurious ultraviolet logarithmic divergence in the physical sector (i.e., for electric and magnetic photons). This divergence is unphysical since in the full theory, including also the non-static photon modes, the q-integral would be cut-off at momenta $q \sim \omega_p$ (recall the discussion in section 2.2). Thus, to be consistent with the approximations performed, we have to complement the above "dimensional reduction" with the prescription that an upper cut-off of the order gT is added in momentum integrals, in the physical sector. Since this cut-off is not exactly known, it will be important in what follows to verify that the physical predictions are independent from its precise value. In the gauge sector, on the other hand, no such cut-off is needed since the corresponding momentum integral turns out to be ultraviolet finite (see below, eq. (4.12)).

Eq. (3.42) determines the large time behavior of the fermion propagator, to be discussed in the next section. At a first sight, the considerable simplifications leading to

27

this equation (and coming from the restriction to the static photon modes in eq. (3.28)) may seem rather accidental. However, as we explain now, there is a simple reason for these simplifications, and, in fact, eq. (3.42) could have been obtained in a more direct way[31], which avoids some of the complications of the Matsubara formalism (the latter are essential only for the non-static modes). Let us indeed return briefly to the functional integral of eq. (3.14), and consider its approximation where the Bloch-Nordsieck propagator $G_E(x, y|A)$ includes only the *static* electromagnetic field $A_\mu(\mathbf{x})$ of eq. (3.37). Then, the contribution of the non-static photon modes to the functional integral trivially factorizes, and is compensated by the corresponding contribution to the partition function Z, thus leaving

$$S_E(x, y) = Z_0^{-1} \int [\mathrm{d}A] \, G_E(x, y|A) \exp \left\{ -\frac{1}{2} \left(A, \, {}^*D^{-1}A \right)_0 \right\}, \qquad (3.44)$$

where $A_\mu \equiv A_\mu(\omega_m = 0, \mathbf{q})$, and $\left(A, {}^*D^{-1}A \right)_0$ denotes the $\omega_m = 0$ contribution to the effective photon action (3.10); correspondingly, Z_0 is the partition function of the static mode alone. Since the background field (3.37) is time-independent, the propagator $G_E(x, y|A)$ depends only on the time difference $x_0 - y_0$, i.e. $G_E(x, y|A) \equiv G_E(x_0 - y_0, \mathbf{x}, \mathbf{y}|A)$. Its Fourier transform can be analytically continued in the complex energy plane, and the resulting function coincides, in the upper half plane, with the retarded propagator. It is then convenient to take the Fourier transform of eq. (3.44), and write ($p^\mu = (i\omega_n, \mathbf{p})$, $\omega_n = (2n + 1)\pi T$):

$$S_E(p) \equiv Z_0^{-1} \int [\mathrm{d}A] \, G_E(\mathbf{x}, p|A) \exp \left\{ -\frac{1}{2} \left(A, \, {}^*D^{-1}A \right)_0 \right\}. \qquad (3.45)$$

Since the energy p_0 enters eq. (3.45) as an external parameter, the continuation to real external energy $p_0 \to \omega + i\eta$, and the Fourier transform to real time, can both be performed *before* doing the functional integration. Thus, the retarded propagator $S_R(t, \mathbf{x})$ can be directly obtained as the functional average of $G_R(x, y|A)$, which is known explicitly (recall eqs. (3.16) and (3.17)).

Specifically, eqs. (3.45) and (3.16) give $S_R(t, \mathbf{p})$ in the form (3.41), where

$$\Delta(t) \equiv Z_0^{-1} \int [\mathrm{d}A] \, U(x, x - vt) \exp \left\{ -\frac{1}{2} \left(A, \, {}^*D^{-1}A \right)_0 \right\}, \qquad (3.46)$$

and the parallel transporter is that of a static background field:

$$\begin{aligned} U(x, x - vt) &= \exp \left\{ -\int \mathrm{d}^3y \, j_\mu(\mathbf{y}) A^\mu(\mathbf{y}) \right\}, \\ j_\mu(\mathbf{y}) &\equiv igv_\mu \int_0^t \mathrm{d}s \, \delta^{(3)}(\mathbf{x} - \mathbf{y} - \mathbf{v}s). \end{aligned} \qquad (3.47)$$

28

A straightforward computation yields then

$$\Delta(t) = \exp\left\{\frac{1}{2}T\int d^3x_1 d^3x_2\, j^\mu(\mathbf{x_1})\,^*D_{\mu\nu}(\mathbf{x_1}-\mathbf{x_2})\,j^\nu(\mathbf{x_2})\right\}$$

$$= \exp\left\{-\frac{g^2}{2}T\int_0^t ds_1 \int_0^t ds_2\,\tilde{\mathcal{D}}(\mathbf{v}(s_1-s_2))\right\}, \qquad (3.48)$$

where

$$\tilde{\mathcal{D}}(\mathbf{x}) \equiv \int \frac{d^3q}{(2\pi)^3}\, e^{i\mathbf{q}\cdot\mathbf{x}}\,\tilde{D}(\mathbf{q}) \qquad (3.49)$$

is the Fourier transform of the static photon propagator (3.43). By using the last equation to perform the s_1 and s_2 integrations, we may cast eq. (3.48) in the form (3.42).

4   The infrared structure of the fermion propagator

4.1   Large time behavior

The non-trivial time dependence of the fermion propagator is contained in the function $\Delta(t)$, eq. (3.42). Because our approximations preserve only the leading infrared behavior of the perturbation theory, eq. (3.42) describes only the leading *large-time* behavior of $\Delta(t)$. Since the only energy scale in the momentum integral of eq. (3.42) is the upper cut-off, of order gT, the large-time regime is achieved for $t \gg 1/gT$.

The expansion of eq. (3.42) in powers of g^2 reproduces the dominant singularities of the usual perturbative expansion for the self-energy. Let us verify this for the correction of order g^2:

$$\delta S_R(\omega,\mathbf{p}) = -g^2 T\, i \int_0^\infty dt\, e^{it(\omega-\mathbf{V}\cdot\mathbf{p}+i\eta)} \int \frac{d^3q}{(2\pi)^3}\frac{\tilde{D}(\mathbf{q})}{(\mathbf{v}\cdot\mathbf{q})^2}\Big(1-\cos t(\mathbf{v}\cdot\mathbf{q})\Big). \qquad (4.1)$$

We perform first the time integration and obtain, after simple algebraic manipulations,[¶]

$$\delta S_R(\omega,\mathbf{p}) = -G_0(\omega,\mathbf{p})\Sigma(\omega,\mathbf{p})\,G_0(\omega,\mathbf{p}), \qquad (4.2)$$

where

$$G_0(\omega,\mathbf{p}) = i\int_0^\infty dt\, e^{it(\omega-\mathbf{V}\cdot\mathbf{p}+i\eta)} = \frac{-1}{\omega-\mathbf{v}\cdot\mathbf{p}+i\eta}, \qquad (4.3)$$

_____

[¶] The self-energy Σ which appears here corresponds to the spin projection Σ_+ of the full self-energy. (See eq. (1.6).)

is the free BN propagator, and

$$\Sigma(\omega, \mathbf{p}) = -g^2 T \int \frac{d^3 q}{(2\pi)^3} \tilde{D}(\mathbf{q}) \frac{-1}{\omega - \mathbf{v} \cdot (\mathbf{p} + \mathbf{q}) + i\eta}. \tag{4.4}$$

The imaginary part of this equation determines the damping rate according to $\gamma = -\mathrm{Im}\,\Sigma(\omega = p)$. We can write, with $\epsilon \equiv \omega - \mathbf{v} \cdot \mathbf{p}$,

$$\begin{aligned}
\mathrm{Im}\,\Sigma(\omega, \mathbf{p}) &= -\pi g^2 T \int \frac{d^3 q}{(2\pi)^3} \delta(\omega - \mathbf{v} \cdot (\mathbf{p} + \mathbf{q}))\, \tilde{D}(\mathbf{q}) \\
&= -\frac{g^2 T}{4\pi} \int_{|\epsilon|}^{\omega_p} dq\, q \left\{ \frac{1}{q^2}\left(1 - \frac{\epsilon^2}{q^2}\right) - \frac{1}{q^2 + m_D^2} + \lambda \frac{\epsilon^2}{q^4} \right\}, \tag{4.5}
\end{aligned}$$

which, in the mass-shell limit $\epsilon \to 0$, and with an IR cut-off μ in the magnetic sector, yields (with $\alpha = g^2/4\pi$)

$$\gamma = \alpha T \left\{ \ln \frac{\omega_p}{\mu} - \frac{1}{2} \ln \left(1 + \frac{\omega_p^2}{m_D^2}\right) + \frac{\lambda - 1}{2} \right\}. \tag{4.6}$$

This first piece inside the parantheses, which comes from the magnetic sector, reproduces the singular piece of the resummed one-loop calculation (recall eq. (2.28)). On the other hand, the other two pieces are not correctly reproduced by the present calculation. The electric piece, which is finite and of the order $g^2 T$, occurs even with a minus sign (recall that the contribution of the electric scattering to the interaction rate in eq. (2.26) was *positive*). The gauge-dependent piece turns out to be non-vanishing, but it could be eliminated by introducing an IR cut-off μ in the gauge sector as well, and by taking the on-shell limit only subsequently [40] (see also the discussion in Appendix B). This situation is generic: our approximation yields correctly only the leading IR divergences of the usual perturbation theory, which all arise from the magnetic sector, but not the subleading terms. In particular, the contributions involving the electric and the gauge sector are subleading, and *should be discarded for consistency.* This is equivalent to using $\tilde{D}(\mathbf{q}) = 1/q^2$ rather than the full static propagator of eq. (3.43).

Let us verify now that the full, non-perturbative, expression of $\Delta(t)$, eq. (3.42), is *free of infrared singularities.* Inspection of the integrand in eq. (3.42) shows that the dominant IR behaviour arises from the limit $|\mathbf{v} \cdot \mathbf{q}| \equiv q \cos \theta \to 0$. This is consistent with the calculations in sections $2.1 - 2.2$ showing that the divergences come from the exchange of magnetic photons emitted or absorbed at nearly 90 degrees. We have, in this limit,

$$\frac{1 - \cos t(\mathbf{v} \cdot \mathbf{q})}{(\mathbf{v} \cdot \mathbf{q})^2} \simeq \frac{t^2}{2} + \mathcal{O}\left(t^4 (\mathbf{v} \cdot \mathbf{q})^2\right), \tag{4.7}$$

and the momentum integral is IR safe, as advertised. We see here, once again, that the gauge dependent piece of the photon propagator (3.43) does not contribute to the leading IR behavior (which is given by the term in $1/q^2$ of the magnetic propagator). Indeed, because of the factor $(\cos\theta)^2$, the gauge propagator $(\cos\theta)^2/q^2$ is less singular as $q\cos\theta \to 0$.

Consider now the UV behavior of the q-integral. This depends logarithmically on the UV cut-off $\sim \omega_p$, and, as a consequence, the large time behavior of $\Delta(t)$ is insensitive to both the precise value of the UV cut-off, and to the specific procedure which is used for its implementation. This will be verified explicitly below.

The evaluation of $\Delta(t)$ is most simply done by using the coordinate space representation (3.48) for $\Delta(t)$. Corresponding to $\tilde{D}(q) = 1/q^2$, we have $\tilde{\mathcal{D}}(\mathbf{x}) = 1/4\pi x$, and we obtain, for $t \gg 1/\omega_p$, $\Delta(t) = \exp(-g^2 T\, F(t))$, with

$$
\begin{aligned}
F(t) &\equiv \frac{1}{2} \int_0^t \mathrm{d}s_1 \int_0^t \mathrm{d}s_2\, \tilde{\mathcal{D}}(\mathbf{v}(s_1 - s_2)) \\
&= \frac{1}{8\pi} \int_0^t \mathrm{d}s_1 \int_0^t \mathrm{d}s_2\, \frac{\theta(|s_1 - s_2| - 1/\omega_p)}{|s_1 - s_2|} \simeq \frac{t}{4\pi}\left(\ln\omega_p t + \mathcal{O}(1)\right).
\end{aligned}
\tag{4.8}
$$

In this calculation, the ultraviolet cut-off has been introduced in the function $\theta(|s_1 - s_2| - 1/\omega_p)$. Let us verify that the same large time behavior is obtained with a different UV regularisation, namely, with the modified photon propagator $\tilde{D}(q) = 1/q^2 - 1/(q^2 + \omega_p^2)$ (Pauli-Villars regularisation). By using

$$
\tilde{\mathcal{D}}(\mathbf{x}) = \int \frac{\mathrm{d}^3 q}{(2\pi)^3}\, \mathrm{e}^{i\mathbf{q}\cdot\mathbf{x}} \left(\frac{1}{q^2} - \frac{1}{q^2 + \omega_p^2}\right) = \frac{1}{4\pi x}\left(1 - \mathrm{e}^{-\omega_p x}\right),
\tag{4.9}
$$

we get successively

$$
\begin{aligned}
F(t) &= \frac{1}{8\pi} \int_0^t \mathrm{d}s_1 \int_0^t \mathrm{d}s_2 \frac{1 - \mathrm{e}^{-\omega_p|s_1 - s_2|}}{|s_1 - s_2|} \\
&= \frac{t}{4\pi}\left\{\frac{1 - \mathrm{e}^{-\omega_p t}}{\omega_p t} - 1 + \int_0^{\omega_p t} \mathrm{d}s\, \frac{1 - \mathrm{e}^{-s}}{s}\right\} \\
&= \frac{t}{4\pi}\left\{\ln\omega_p t + (\gamma_E - 1) + \frac{1 - \exp(-\omega_p t)}{\omega_p t} + \mathrm{E}_1(\omega_p t)\right\},
\end{aligned}
\tag{4.10}
$$

where $\mathrm{E}_1(x)$ is the exponential-integral function, $\mathrm{E}_1(x) = \int_1^\infty \mathrm{d}y\,(\mathrm{e}^{-xy}/y)$, and γ_E the Euler constant. At very large times, $\omega_p t \gg 1$, we may use the asymptotic expansion of the exponential-integral to get, for the r.h.s. of eq. (4.10),

$$
F(t) \simeq (t/4\pi)\left(\ln\omega_p t + (\gamma_E - 1)\right) \simeq (t/4\pi)\ln\omega_p t,
\tag{4.11}
$$

which coincides, as long as the leading logarithm is concerned, with the previous result (4.8). On the other hand, the subleading term, i.e. the constant under the logarithm, is dependent on the UV regularisation. Thus, as expected, it is only the dominant behavior at very large times which is consistently described by our approximation; the subleading terms should be ignored.

We have argued before that the gauge-fixing terms are not important to the order of interest. To verify this explicitly, we compute the gauge-dependent contribution to $F(t)$, as given by the last term of the photon propagator (3.43):

$$\delta F(t) \equiv \lambda \int \frac{d^3 q}{(2\pi)^3} \frac{(\mathbf{v} \cdot \mathbf{q})^2}{q^4} \frac{1 - \cos t(\mathbf{v} \cdot \mathbf{q})}{(\mathbf{v} \cdot \mathbf{q})^2} = \lambda \frac{t}{8\pi}. \tag{4.12}$$

At large times, this is indeed subleading with respect to (4.11). Note that, the momentum integral in eq. (4.12) being ultraviolet finite, no upper cut-off has been necessary in its evaluation.

We conclude that, at times $t \gg 1/\omega_p$, the function $\Delta(t)$ is gauge-independent and of the form $(\alpha = g^2/4\pi)$

$$\Delta(\omega_p t \gg 1) \simeq \exp\left(-\alpha T t \ln \omega_p t\right). \tag{4.13}$$

The most striking feature of this result is the fact that, at very large times $(\omega_p t \to \infty)$, the fermion propagator is decreasing faster than any exponential. We also note that the scale of the time variations is fixed by the plasma frequency $\omega_p \sim gT$.

A measure of the decay time τ is given by

$$\frac{1}{\tau} = \alpha T \ln \omega_p \tau = \alpha T \left(\ln \frac{\omega_p}{\alpha T} - \ln \ln \frac{\omega_p}{\alpha T} + ... \right). \tag{4.14}$$

Since $\alpha T \sim g\omega_p$, we see that $\tau \sim 1/(g^2 T \ln(1/g))$. This is very close to the perturbative result (2.28), which, in the presence of an IR cut-off $\sim g^2 T$, predicts a damping rate $\gamma \sim g^2 T \ln(1/g)$. A comparison of the two decay laws, $\Delta(t) = \exp(-g^2 T F(t))$, with $F(t)$ from eq. (4.10), and the exponential[‖] $\Delta_L(t) = \exp(-\gamma t)$ with $\gamma = \alpha T \ln(1/g)$, is presented in Fig. 7 for $g = 0.4$. In this figure, the time is measured in units of $1/\omega_p$, and the results displayed for $\Delta(t)$ can be trusted for values $\omega_p t >> 1$, where our approximations are expected to hold. For very large times, $t \gg \tau$, the function $\Delta(t)$ is indeed more rapidly decreasing than the exponential $\Delta_L(t)$. On the other hand, for intermediate, but still

---

[‖] This is the spectral function which would produce an exponential decay in time with a lifetime as close as possible to the nonperturbative result (4.14).
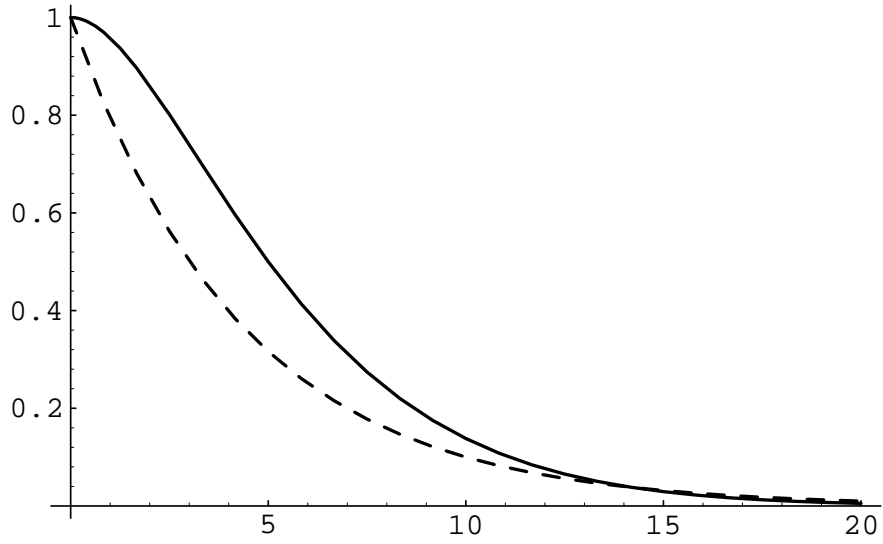
Figure 7: The time behavior of the fermion propagator as described by the nonperturbative result $\Delta(t)$ (full line) and by the exponential $\Delta_L(t)$ (dashed line) for $g = 0.4$. On the abscissa axis, time is measured in units of $1/\omega_p$.

large, times, $1/gT \ll t \ll 1/g^2T$, the opposite situation holds: $\Delta(t) > \Delta_L(t)$. When discussing the lifetime of the excitation, it is rather the intermediate range of times which matters, since for asymptotically large times $t \gtrsim 1/g^2T$ the excitation has already decayed. It follows that, for the range of times of interest, the decay of the excitation is actually *slower* than the one predicted by perturbation theory.

4.2 Mass-shell behavior

The non-trivial large-time behavior exhibited in eq. (4.13) has interesting consequences on the behavior of the retarded propagator in the complex energy plane. In fact, since at large times $\Delta(t)$ is decreasing faster than any exponential, the time-integral giving the Fourier transform

$$S_R(\omega, \mathbf{p}) = \int_{-\infty}^{\infty} \mathrm{d}t \, \mathrm{e}^{-i\omega t} S_R(t, \mathbf{p}) = i \int_0^{\infty} \mathrm{d}t \, \mathrm{e}^{it(\omega - \mathbf{v}\cdot\mathbf{p} + i\eta)} \Delta(t), \qquad (4.15)$$

is absolutely convergent for *any* complex (and finite) ω. That is, the retarded propagator $S_R(\omega)$ is an entire function, with sole singularity at $\mathrm{Im}\,\omega \to -\infty$. Recall, however, that strictly speaking, our present approximation holds only in the vicinity of the mass-shell. Therefore, when speaking about $|\omega - \mathbf{v}\cdot\mathbf{p}| \to \infty$ we have in mind off-shell deviations which are much larger than g^2T. To further clarify this point, let us give a crude estimate of how $S_R(\omega)$ increases as $\mathrm{Im}\,\omega \to -\infty$. To this aim, let us consider $\omega = \mathbf{v}\cdot\mathbf{p} - i\zeta$, with real and positive ζ. We write:

$$S_R(\zeta) = i \int_0^{\infty} \mathrm{d}t \, \mathrm{e}^{\zeta t} \Delta(t), \qquad (4.16)$$

which is a purely imaginary function of ζ, and consider the behaviour of $|S_R(\zeta)|$ for $\zeta \gg \alpha T$. Regarded as a function of t, the integrand $\mathrm{e}^{\zeta t} \Delta(t)$ is rapidly increasing for small t, but it is decreasing for sufficiently large values of t, where the decay of $\Delta(t)$ starts to dominate. Assuming the time integral in (4.16) to be dominated by large values of t, — which is correct for large enough ζ —, we can use the asymptotic expression (4.13), and determine the time t^* at which the integrand is maximum:

$$\omega_p t^* = \exp \frac{\zeta - \alpha T}{\alpha T}. \qquad (4.17)$$

By using the fact that the integrand is positive definite, and that, according to eq. (4.17), $\zeta - \alpha T \ln \omega_p t^* = \alpha T$ and thus $\zeta - \alpha T \ln \omega_p t > \alpha T$ for any $t < t^*$, we can write[**]

$$|S_R(\zeta)| \; > \; \int_0^{t^*} \mathrm{d}t \, \mathrm{e}^{\alpha T t} \; = \; \frac{1}{\alpha T} \left(\exp(\alpha T t^*) - 1 \right), \tag{4.18}$$

so that

$$|S_R(\zeta)| > \frac{1}{\alpha T} \left\{ \exp \left(\tilde{g} \exp \frac{\zeta - \alpha T}{\alpha T} \right) - 1 \right\} \simeq \frac{1}{\alpha T} \exp \left(\tilde{g} \exp \frac{\zeta}{\alpha T} \right), \tag{4.19}$$

where $\tilde{g} \equiv \alpha T / \omega_p = (3/4\pi) \, g$. Eq. (4.19) shows that $|S_R(\zeta)|$ is rapidly increasing starting with values of ζ such that $\tilde{g} e^{\frac{\zeta}{\alpha T}} \sim 1$, that is, $\zeta \sim \alpha T \ln(1/g)$. In perturbation theory, $S_R(\omega)$ has a pole at $\omega = \mathbf{v} \cdot \mathbf{p} - i\gamma$, where $\gamma \simeq \alpha T \ln(\omega_p/\mu) \simeq \alpha T \ln(1/g)$ if $\mu \sim g^2 T$. Thus, our non-perturbative solution for $S_R(\omega)$ replaces the pole at finite distance by an essential singularity at $-i\infty$, which however starts manifesting itself at distances $\sim g^2 T \ln(1/g)$ below the real axis, that is, at the same distances as the pole of the perturbation theory.

Since $S_R(\omega)$ is analytic in any finite neighbourhood of the tree-level mass-shell at $\omega = \mathbf{v} \cdot \mathbf{p}$, we need to clarify the mass-shell interpretation. To this aim, we consider the spectral density $\acute{\rho}(\omega, \mathbf{p})$

$$\acute{\rho}(\omega, \mathbf{p}) = 2 \operatorname{Im} S_R(\omega, \mathbf{p}) = 2 \int_0^\infty \mathrm{d}t \, \cos t(v \cdot p) \, \Delta(t), \tag{4.20}$$

where $v \cdot p = \omega - \mathbf{v} \cdot \mathbf{p}$. It satisfies the sum-rule[††]

$$\int_{-\infty}^\infty \frac{\mathrm{d}\omega}{2\pi} \, \acute{\rho}(\omega, \mathbf{p}) = \Delta(t = 0) = 1. \tag{4.21}$$

We have calculated $\acute{\rho}(\omega, \mathbf{p})$ numerically, and the result is plotted, for a coupling constant $g = 0.08$, in Fig. 8. We also represent, for the same value of g, the Lorentzian spectral function ($\epsilon \equiv v \cdot p$)

$$\rho_L(\epsilon) \; = \; \frac{2\gamma}{\epsilon^2 + \gamma^2}, \tag{4.22}$$

with $\gamma = \alpha T \ln(1/g)$. This is the spectral function which would produce the exponential time decay $\Delta_L(t) = \exp(-\gamma t)$ alluded to at the end of the previous subsection. It is seen on these figures that, in the weak coupling limit, the spectral density $\acute{\rho}(\epsilon)$ has the

---

[**]This estimate was suggested to us by A. Rebhan [52]

[††]In fact, this sum rule holds exactly in the Bloch-Nordsieck model, independently of the restriction to the static photon mode. In general, $\Delta(t = 0)$ is replaced, in eq. (4.21), by $S^>(t = 0, \mathbf{p}) + S^<(t = 0, \mathbf{p})$, which is also equal to one, as shown by eq. (3.35).
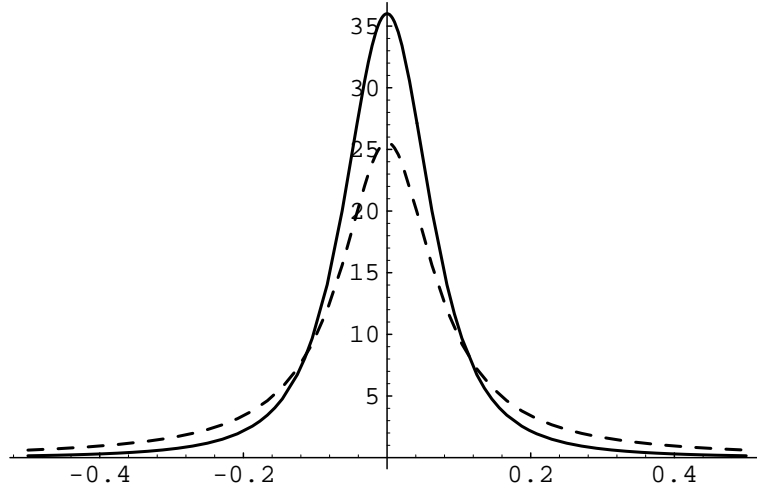
Figure 8: The spectral density $\acute{\rho}(\epsilon)$ (full line, in units of $1/\omega_p$) and the lorentzian $\rho_L(\epsilon)$ (dashed line) for $g = 0.08$, as a function of $\epsilon \equiv v \cdot p$ in units of ω_p.

shape of a *resonance* strongly peaked around $\epsilon = 0$, and with a typical witdh of the order $1/\tau \sim g^2 T \ln(1/g)$, that is, of the same order as that of the Lorentzian. This allows us to identify the mass-shell of the full propagator at $\omega = \mathbf{v} \cdot \mathbf{p}$, as at treel-level. Moreover, it is clear from Fig. 8 that, for very small $g \ll 1$, the nonperturbative spectral density is even *sharper* than a Lorentzian. Thus the net result of the infrared effects considered here is to slightly *enhance* the stability of the quasiparticle state (see also the discussion at the end of the previous subsection).

Finally, it is interesting to compute the imaginary part of the exact self-energy, by inverting the Dyson-Schwinger equation $S_R^{-1}(\omega, \mathbf{p}) = -(\omega - \mathbf{v} \cdot \mathbf{p}) + \Sigma_R(\omega, \mathbf{p})$. A simple calculation yields

$$-\,\mathrm{Im}\Sigma_R(\epsilon) \;=\; \frac{2\acute{\rho}(\epsilon)}{\acute{\sigma}^2(\epsilon) + \acute{\rho}^2(\epsilon)}\,, \tag{4.23}$$

where $\epsilon \equiv v \cdot p$, $\acute{\rho}(\epsilon)$ is the spectral density of eq. (4.20) and

$$\acute{\sigma}(\epsilon) \equiv 2 \int_0^\infty \mathrm{d}t \, \sin \epsilon t \, \Delta(t). \tag{4.24}$$

This is represented graphically in Fig. 9, together with the pure one-loop result, eq. (4.5),
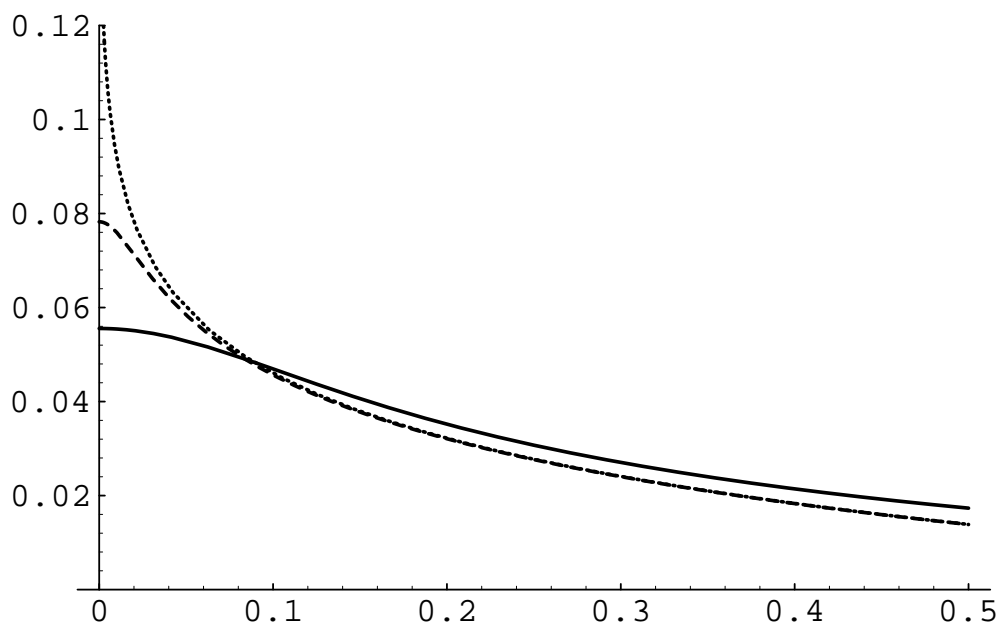
36

Figure 9: The imaginary part of the self-energy, eq. (4.23), as a function of the energy, for $g = 0.08$: nonperturbative calculation (full line), one-loop result (dotted line) and one-loop result in the presence of an IR cut-off $\sim g^2 T$ (dashed line). All the quantities are measured in units of ω_p.

which shows a logarithmic divergence as $\epsilon \to 0$ (dotted line), and the screened one-loop result, as obtained from eq. (4.4) after inserting an IR cut-off equal to αT (dashed line). As manifest on this figure, the full result for $\text{Im}\,\Sigma_R$ is finite at the mass-shell $\epsilon = 0$, and inferior to the value predicted by the perturbation theory with an IR cut-off $\sim g^2 T$. The latter property is consistent with the the previous analysis of the spectral density, and also of the time behavior at intermediate times. One can also verify the non perturbative character of the solution. For example, $\text{Im}\,\Sigma_R(\epsilon = 0) = -1/\int_0^\infty dt\,\Delta(t)$ has no expansion in powers of g^2 even if one keeps ω_p constant in eq. (4.13) for $\Delta(t)$.

5   The lifetime of the soft fermionic excitations

For soft momenta, $p \sim gT$, the quasiparticles become collective excitations, with non-trivial dispersion relations[1, 2] and self-interactions[4, 5]. To leading order in g, the dispersion relations are real, and the quasiparticles propagate without damping. At next to leading order, collisional damping occurs. The corresponding damping rate γ has been calculated in the effective (i.e., HTL-resummed) perturbation theory[4]. For an excitation with zero momentum ($p = 0$), γ is finite and of the order $g^2 T$ [4, 8]. However, for excitations with finite momentum $p \gg g^2 T$, the lowest order perturbative calculation of γ meets with the same infrared problem as that discussed for the hard particles[18, 25]. As we shall see, this problem is solved by the same technique as that used for the hard fermion.

5.1   The HTL approximation

Let us recall first the main features of the dispersion relations for soft fermions, to leading order in g. They are obtained from the poles of the effective propagator $^*S(\omega, \mathbf{p})$ which is obtained as $^*S^{-1} = S_0^{-1} + \delta\Sigma$, with $\delta\Sigma(\omega, \mathbf{p})$ denoting the fermion self-energy in the HTL approximation[1, 2]:

$$\delta\Sigma(\omega, \mathbf{p}) = \omega_0^2 \int \frac{d\Omega}{4\pi} \frac{\not{v}}{\omega - \mathbf{v} \cdot \mathbf{p} + i\eta}. \tag{5.1}$$

In this equation, $\omega_0 = gT/\sqrt{8}$ is the frequency of the spatially uniform ($p = 0$) fermionic excitations. The propagator is conveniently written in the form (1.7), that is,

$$^*S(\omega, \mathbf{p}) = {}^*\Delta_+(\omega, p) h_+(\hat{\mathbf{p}}) + {}^*\Delta_-(\omega, p) h_-(\hat{\mathbf{p}}), \tag{5.2}$$

38

where

$$^*\Delta_\pm(\omega, p) = \frac{-1}{\omega \mp (p + \delta\Sigma_\pm(\omega, p))}, \tag{5.3}$$

and

$$\delta\Sigma_\pm(\omega, p) = \pm\frac{1}{2}\,\mathrm{tr}\left(h_\pm(\hat{\mathbf{p}})\delta\Sigma(\omega, \mathbf{p})\right). \tag{5.4}$$

The pole equations $^*\Delta_\pm^{-1}(\omega(p), p) = 0$ yield two positive energy branches $\omega_\pm(p)$ [1], instead of the usual one (with $\omega = p$) in the free electron spectrum. For ω close to the mass-shell at $\omega_s(p)$, $s = \pm$, we can write

$$^*\Delta_s(\omega, \mathbf{p}) \simeq \frac{z_s(p)}{\omega_s(p) - \omega}, \tag{5.5}$$

where $z_s(p)$ is the residue of the mode s,

$$z_s^{-1}(p) = 1 - \frac{\partial\,\delta\Sigma_s(\omega, p)}{\partial\omega}\bigg|_{\omega=\omega_s(p)}. \tag{5.6}$$

Since $\omega_\pm(p) > p$ for any p, both dispersion relations are real: the quasiparticles propagate without damping in this approximation. For small momenta, $p \ll gT$, $\omega_\pm(p) \simeq \omega_0 \pm p/3$. The upper branch is strictly increasing ($v_+(p) > 0$ for any p), while the lower branch has a minimum at $p = p_c \approx 0.92\,\omega_0$. At very large momenta, $p \gg \omega_0$, both branches approach the light cone, but $z_+(p) \to 1$, while $z_-(p)$ vanish exponentially. (See Refs. [10, 12, 13] for more details and physical interpretation.)

Because of the gauge symmetry, the nonlocal character of the HTL self-energy (5.1) leads to effective interactions between a fermion pair and any number of soft photons. For instance, the Ward identity

$$q^\mu\,^*\Gamma_\mu(p, p + q) = \,^*S^{-1}(p) - \,^*S^{-1}(p + q), \tag{5.7}$$

requires the existence of a nonlocal 3-point vertex function, which is indeed found in the form $^*\Gamma_\mu(p, p + q) = \gamma_\mu + \delta\Gamma_\mu(p, p + q)$, where $\delta\Gamma_\mu(p, p + q)$ is the 3-point HTL [4, 5]:

$$\delta\Gamma_\mu(p, p + q) = \omega_0^2 \int \frac{d\Omega}{4\pi} \frac{v_\mu \slashed{v}}{(v \cdot p + i\eta)(v \cdot (p + q) + i\eta)}. \tag{5.8}$$

Similarly, higher vertices, without analogue at the tree-level, are necessary in order to fulfill the higher order Ward identities. We show here one more example, namely the Ward identity satisfied by the 2-fermions — 2-photons vertex function:

$$q_1^\mu\,^*\Gamma_{\mu\nu}(p_1, p_2; q_1, q_2) = \,^*\Gamma_\nu(p_1, p_1 + q_2) - \,^*\Gamma_\nu(p_1 + q_1, p_1 + q_1 + q_2), \tag{5.9}$$
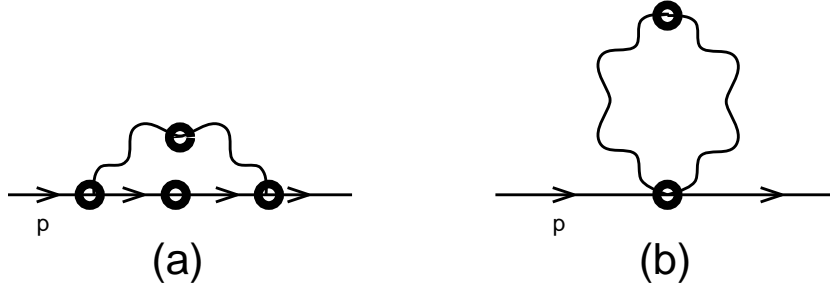
Figure 10: One-loop diagrams for the soft fermion self-energy in the effective expansion.

where, in the left hand side, p_i and q_i are respectively the momenta of the incoming fermions and photons, with $p_1 + p_2 + q_1 + q_2 = 0$. For what follows, it is important to remark that all the HTL vertex functions are (almost) uniquely determined by the self-energy (5.1) and the Ward identities like eq. (5.7) [5, 47]. This is so since the non-linear structure of the effective action of the HTL's is the minimal one which is consistent with the gauge symmetry[5, 48, 11].

5.2 Perturbation theory for the damping rate

In this section, we discuss the perturbative computation of the damping rate for the soft fermion, and the related IR problems. After a brief summary of the leading-order computation [4, 18, 25], we discuss higher orders corrections and how they simplify in the computation of the leading divergent terms.

The dominant contribution to the damping rate, of order $g^2 T$, comes from the imaginary part of the (resummed) one-loop self-energy $^*\Sigma(\omega, \mathbf{p})$, as given by the two diagrams in Fig. 10 [4]. Specifically,

$$\gamma_\pm(p) = -z_\pm(p) \operatorname{Im} {}^*\Sigma_\pm(\omega_\pm(p) + i\eta, p), \tag{5.10}$$

where $^*\Sigma_\pm(p) = \operatorname{tr}(h_\pm(\hat{\mathbf{p}})^*\Sigma(p))/2$ and the subscripts $\pm$ refer to the two positive-energy modes in the fermion spectrum. Note that, in general, the "tadpole" diagram in Fig. 10.b gives a non-trivial contribution to γ, since the 4-point vertex itself has a non-zero discontinuity. Moreover, the imaginary part of the diagram in Fig. 10.a comes not only from the cutting of the internal propagators (as for the usual one-loop diagram discussed in section 2), but also from the discontinuity of the resummed 3-point vertices.

In what follows, we concentrate on the singular contribution to γ. This comes

entirely from the diagram in Fig. 10.a [18], which reads

$$^*\Sigma_a(p) = -g^2 T \sum_{q^0=i\omega_m} \int \frac{\mathrm{d}^3 q}{(2\pi)^3} {}^*\Gamma_\mu(p, p+q) {}^*S(p+q) {}^*\Gamma_\nu(p+q, p) {}^*D^{\mu\nu}(q). \quad (5.11)$$

It has been already recognized[18] that the singular piece of γ arises from the same kinematical regime as for a hard fermion, namely, from the exchange of a very soft ($q \lesssim g^2 T$) magnetic photon at nearly 90 degrees. This allows for kinematical approximations identical to those encountered in section 2. In particular, the whole singularity can be reproduced by restricting the calculation to the *magnetostatic* mode $q^0 = i\omega_m = 0$ [25], with propagator $^*D^{ij}(\omega_m = 0, \mathbf{q}) = \delta^{ij}/q^2$, and with an upper cut-off $\sim gT$. Furthermore, the internal fermion propagator $^*S(\omega, \mathbf{p} + \mathbf{q})$ is nearly on-shell, since $\omega \simeq \omega_\pm(p)$, and $q \ll p$. Thus we can write $\omega_\pm(\mathbf{p} + \mathbf{q}) \simeq \omega_\pm(p) + \mathbf{v}_\pm(p) \cdot \mathbf{q}$, — where $\mathbf{v}_s(p)$ denotes the group velocity of the mode s, $\mathbf{v}_s(p) \equiv \partial\omega_s(p)/\partial\mathbf{p} = v_s(p)\hat{\mathbf{p}}$ —, and replace $^*S(\omega, \mathbf{p} + \mathbf{q}) \longrightarrow {}^*\Delta_\pm(\omega, \mathbf{p} + \mathbf{q})h_\pm(\hat{\mathbf{p}})$, with (recall eq. (5.5))

$$^*\Delta_\pm(\omega, \mathbf{p} + \mathbf{q}) \simeq \frac{-z_\pm(p)}{\omega - \omega_\pm(p) - \mathbf{v}_\pm(p) \cdot \mathbf{q}}, \quad (5.12)$$

where the upper (lower) sign applies according to whether the external line is close to the mass-shell of the upper branch, or of the lower branch, respectively. A final simplification refers to the 3-point vertex function $^*\Gamma^i(\mathbf{p}, \mathbf{p} + \mathbf{q})$, where we can neglect the photon momentum $\mathbf{q}$ and use the differential form of the Ward identity (5.7) to write:

$$^*\Gamma^i(\mathbf{p}, \mathbf{p}) = \frac{\partial\,^*S^{-1}(\omega, \mathbf{p})}{\partial p^i}. \quad (5.13)$$

(The dependence of the vertex function on the external energy ω is not indicated explicitly.) The inverse propagator is conveniently written as (recall eq. (1.7))

$$^*S^{-1}(\omega, \mathbf{p}) = {}^*\Delta_+^{-1}(\omega, p)h_-(\hat{\mathbf{p}}) + {}^*\Delta_-^{-1}(\omega, p)h_+(\hat{\mathbf{p}}). \quad (5.14)$$

From eqs. (5.13) and (1.7), we obtain, for $\omega \simeq \omega_\pm(p)$,

$$\begin{aligned}
h_\pm(\hat{\mathbf{p}})^*\Gamma^i(\mathbf{p}, \mathbf{p})h_\pm(\hat{\mathbf{p}}) &= h_\pm(\hat{\mathbf{p}}) \frac{\partial\,^*\Delta_\pm^{-1}}{\partial p^i} \simeq h_\pm(\hat{\mathbf{p}}) \frac{v_\pm^i(p)}{z_\pm(p)} \\
\mathrm{tr}\left(h_\pm(\hat{\mathbf{p}})^*\Gamma^i(\mathbf{p}, \mathbf{p})\right) &= 2\frac{\partial\,^*\Delta_\pm^{-1}}{\partial p^i} \simeq 2\frac{v_\pm^i(p)}{z_\pm(p)}.
\end{aligned} \quad (5.15)$$

The particular spin projections of $^*\Gamma^i$ written down above are the only ones which enter $^*\Sigma_\pm \equiv \mathrm{tr}\,(h_\pm{}^*\Sigma)/2$, and therefore the damping rate (5.10).

41

Note that the simplified vertex (5.15) has no discontinuity, so that the whole imaginary part of $^*\Sigma$ in the kinematical regime of interest arises by cutting the internal lines in Fig. 10.a. Specifically, the previous approximations yield the dominant (infrared singular) piece of the one-loop damping rate as[18, 25]

$$
\begin{aligned}
\gamma_\pm(p) &\simeq z_\pm g^2 T \int \frac{\mathrm{d}^3 q}{(2\pi)^3} \frac{v_\pm^i}{z_\pm} \frac{\delta^{ij}}{q^2} \frac{v_\pm^j}{z_\pm} \mathrm{Im} \frac{-z_\pm}{\omega - \omega_\pm(p) - |v_\pm| q \cos\theta + i\eta} \\
&\simeq \alpha T |v_\pm(p)| \ln \frac{\omega_p}{|\omega - \omega_\pm(p)|},
\end{aligned}
\tag{5.16}
$$

which is very close to eq. (2.31) for a hard fermion (recall that $|\mathbf{v}| = 1$ for the hard quasiparticle).

Consider now the higher order corrections to γ, with emphasis on the leading infrared contributions. By relying mostly on the gauge symmetry, we argue now that the most singular contributions to γ arise from multi-loop diagrams which involve the (resummed) 3-point photon-fermion vertex, *but not the higher order vertices*[‡‡]. This is so since in the kinematical regime of interest, the inverse fermion propagator,

$$
^*\Delta_s^{-1}(\omega, \mathbf{p} + \mathbf{q}) \simeq -\left(\omega - \omega_s(p) - \mathbf{v}_s(p) \cdot \mathbf{q}\right) \frac{1}{z_s(p)},
\tag{5.17}
$$

is *linear* in the photon momentum $\mathbf{q}$, so that the Ward identity (5.7) can be satisfied by a 3-point vertex $^*\Gamma^i(\mathbf{p}, \mathbf{p} + \mathbf{q})$ which is *independent* of the momentum of the photon leg. And we have seen indeed that the singular one-loop contribution is obtained by replacing $^*\Gamma^i(\mathbf{p}, \mathbf{p} + \mathbf{q})$ with $^*\Gamma^i(\mathbf{p}, \mathbf{p})$, which is independent of $\mathbf{q}$ and (up to a spin projector) equal to $v_s^i(p)/z_s(p)$. Furthermore, with a $\mathbf{q}$-independent 3-point vertex, all the other, higher, Ward identities — as the one shown in eq. (5.9) — are trivially satisfied by setting the n-point HTL's with $n \geq 4$ to zero. Since, as alluded to before, the vertex HTL's are essentially determined by the Ward identities, it follows that the higher-point vertices (beyond the 3-point function) are not important in the kinematical regime of interest.

We thus conclude that, in order to isolate the most singular contributions to γ_s ($s = \pm$) in perturbation theory, we have to consider the *same* diagrams as for the hard fermion, and evaluate them with the following simplified Feynman rules:

(i) the photon propagator $D_0^{ij}(\mathbf{q}) = \delta^{ij}/q^2$;

(ii) the fermion propagator $^*\Delta_s(\omega, \mathbf{p} + \mathbf{q})$ from eq. (5.12);

[‡‡]This can be also verified by power counting, as in Ref. [18] for the one-loop calculation. Namely, cutting a vertex rather than a fermion propagator, yields a factor of $1/(\mathbf{v}_s(p) \cdot \mathbf{q})$ less, and thus a less singular infrared behavior.

(iii) the photon-fermion vertex ${}^*\Gamma^i_s(p) = v^i_s(p)/z_s(p)$.

The momentum integrals over the photon momenta should be computed with an upper cut-off of the order ω_p. Strictly speaking, the above simplifications hold only for very soft momenta, $q \ll p \sim gT$, and not up to momenta $q \sim \omega_p$. This is not important, however, since the dominant (singular) contributions arise from the limit $q \to 0$ and are insensitive to the upper cut-off.

Note that the above Feynman rules are essentially those of a *local* effective field theory, in contrast with the general HTL Feynman rules, which are non-local. (The apparent dependence on ω and p is irrelevant here, since these are the *fixed* energy and momentum of the external line; they enter the computation as parameters). Furthermore, the IR contribution to γ is largerly insensitive to the details of the HTL resummation, which enters only via the global factors $v_s(p)$ and $z_s(p)$. Actually, to the order of interest, γ_s is even independent of the residue $z_s(p)$, as also suggested by the one-loop result (5.16). This is so since a general n-loop graph contributing to Σ_s (in the simplified perturbation theory introduced above) involves $2n$ vertices ${}^*\Gamma^i_s$, and therefore a factor z_s^{-2n}, and $(2n-1)$ propagators ${}^*\Delta_s$, which yield a factor z_s^{2n-1}. The remaining factor of $1/z_s$ disappears in the computation of $\gamma_s = -z_s \mathrm{Im}\, \Sigma_s$.

5.3   The Bloch-Nordsieck model for a soft fermion

At this point, the analysis of the dominant mass-shell behavior of the soft fermion becomes almost identical to the corresponding analysis for the hard fermion. This this analogy is due to the fact that the soft photons responsible for the IR divergences have typical momenta $q \ll gT$, which are much smaller than the momentum $p \sim gT$ of the soft fermion. In view of this, the whole discussion in sections 3 and 4 can be directly extended to the case of a soft fermion.

Specifically, the simplified Feynman rules which apply in the IR regime are, once again, those of the Bloch-Nordsieck model, and can be summarized in the following functional integral representation of the soft fermion propagator:

$$S_\pm(x,y) = Z_0^{-1} \int [\mathrm{d}\mathbf{A}] \, G_\pm(x,y|\mathbf{A}) \exp\left\{ -\frac{1}{2} \left(\mathbf{A}, D_0^{-1}\mathbf{A} \right)_0 \right\}. \tag{5.18}$$

In this equation, $G_s(x,y|\mathbf{A})$ is the Bloch-Nordsieck propagator for the quasiparticle in the mode s, $s = \pm$, in the presence of the static magnetic field $A^\mu = (0, \mathbf{A}(\mathbf{x}))$, and satisfies

(with $v_s^\mu \equiv (1, \mathbf{v}_s)$)

$$-i \, (v_s \cdot D_x) \, G_s(x, y | A) \;\; = \;\; z_s \, \delta^{(4)}(x - y). \tag{5.19}$$

Furthermore,

$$\left(\mathbf{A}, D_0^{-1} \mathbf{A}\right)_0 \;\; = \;\; \frac{1}{T} \int \mathrm{d}^3 x \, \mathrm{d}^3 y \, A^i(\mathbf{x}) \, D_{0\,ij}^{-1}(\mathbf{x} - \mathbf{y}) A^j(\mathbf{y}), \tag{5.20}$$

where the vector field $A^i(\mathbf{x})$ has been defined in eq. (3.37), and $D_{0\,ij}(\mathbf{x}) = \delta_{ij}/4\pi x$. Note that the free (retarded) BN propagator, as obtained from eq. (5.19) with $A = 0$, reads

$$G_s(\omega, \mathbf{p} + \mathbf{q}) \;\; = \;\; \frac{-z_s}{\omega - \mathbf{v_s} \cdot (\mathbf{p} + \mathbf{q}) + i\eta} \,. \tag{5.21}$$

Strictly speaking, the mass-shell for the BN particle of momentum p, that is $\omega = \mathbf{v_s} \cdot \mathbf{p}$, is different from the real leading-order mass-shell, at $\omega = \omega_s(p)$. This is so, of course, since the dispersion relations for soft fermions are not linear, so that the group velocity $|\mathbf{v_s}|$ is really momentum dependent. However, this difference is not important, since the BN propagator (5.21) presents the correct dependence on $\mathbf{q}$ in the mass-shell limit. Compare in this respect eqs. (5.21) and (5.12): in both these equations, it is the difference in energy with respect to the mass-shell which matters, rather than the precise value of the mass-shell energy itself. For $\omega = \omega_s(p)$ in eq. (5.12), and respectively for $\omega = \mathbf{v_s} \cdot \mathbf{p}$ in eq. (5.21), the propagators in these two equations become identical.

Eqs. (5.18)–(5.19) are further manipulated as in section 3.5 (recall, especially, the discussion after eq. (3.44)). As a result, we obtain the retarded propagator for the two fermionic modes $\pm$, for momenta $p \sim gT$ and energies close to the mass-shell, $\omega \simeq \omega_\pm(p)$. It reads

$$S_\pm(\omega, \mathbf{p}) \;\; = \;\; i \, z_\pm(p) \int_0^\infty \mathrm{d}t \, e^{it(\omega - \omega_\pm(p) + i\eta)} \, \Delta_\pm(t),$$

$$\Delta_\pm(t) \;\; = \;\; \exp\left\{-g^2 T \int \frac{\mathrm{d}^3 q}{(2\pi)^3} \frac{\tilde{D}_\pm(\mathbf{q})}{(\mathbf{v_\pm} \cdot \mathbf{q})^2} \left(1 - \cos t(\mathbf{v_\pm} \cdot \mathbf{q})\right)\right\}. \tag{5.22}$$

In this equation, $\tilde{D}_\pm(\mathbf{q}) = v_\pm^i D_0^{ij}(\mathbf{q}) v_\pm^j = v_\pm^2/q^2$, so that we can write

$$\Delta_\pm(t) = \;\; \Delta(|v_\pm| t), \tag{5.23}$$

with $\Delta(t)$ as given by eq. (3.42) where $\tilde{D}(\mathbf{q}) \to 1/q^2$ and $\mathbf{v}$ is an arbitrary unit vector. Note that the functions $\Delta_\pm(t)$ are implicitly dependent on the momentum p, via the group velocities $v_\pm(p)$. Both the mass-shell behavior of the propagator (5.22) and the large time

44

behavior of the propagator $S_\pm(t, \mathbf{p})$ follows from the analysis in section 4. At very large times $\omega_p |v_\pm| t \gg 1$, we have

$$\Delta_\pm(\omega_p |v_\pm| t \gg 1) \simeq \exp\left\{-\alpha T |v_\pm| t \ln(\omega_p |v_\pm| t)\right\}. \tag{5.24}$$

The spectral density of the mode s is peaked around $\omega = \omega_s(p)$, with a width of the order $g^2 T |v_s| \ln(1/g)$. In particular, for the lower mode $\omega_-(p)$, and for $p = p_c$, where $v_-(p_c) = 0$, eq. (5.23) shows that, to this approximation, the "plasmino" mode is not damped, in accordance with the one-loop result for the damping rate, eq. (5.16).

6   Conclusions

The analysis presented in this paper suggests that the damping of the fermionic excitations with momenta $p \gg g^2 T$ is *not* exponential in time, but of the more complicated form $S_R(t) \sim e^{-iE(p)t} \exp\{-\alpha T |v| t \ln(\omega_p |v| t)\}$, where $\mathbf{v} = \partial E / \partial \mathbf{p}$ is the group velocity of the excitation, $\omega_p \sim gT$ is the plasma frequency, and $\alpha = g^2/4\pi$. As a consequence, the retarded propagator $S_R(\omega)$ has no quasiparticle pole, but the spectral density shows nevertheless a sharp resonance peaked at $\omega = E(p)$, with a width $\sim g^2 T \ln(1/g)$. At the present level of accuracy, the mean energy $E(p)$ is given by the leading-order approximation, namely $E(p) = p$ for a hard excitation, and $E(p) = \omega_\pm(p)$ for a soft one. We note that this result solves the IR problem of the damping rate in a very "soft" way, by essentially replacing the IR cut-off μ in the perturbative result $\Delta_L(t) = \exp\{-\alpha T |v| t \ln(\omega_p |v|/\mu)\}$ with the inverse of the time. Thus, quantitatively, the lifetime of the excitation does not differ much from that obtained from leading-order perturbation theory.

The asymptotic behaviour of the retarded propagator has been obtained by solving exactly an effective theory which reproduces all the leading infrared divergences of the perturbation theory. The physical processes which are responsible for these divergences are the multiple collisions involving the exchange of long wavelength, quasi-static, magnetic photons, which are not screened by plasma effects. By comparison, the longitudinal, gauge sector is less singular in perturbation theory, and does not contribute to the dominant large time behaviour of the non-perturbative solution.

At finite temperature, the presence of the thermal bath amplifies the IR divergences, in such a way that they become effectively those of a three-dimensional gauge theory. Then, a comparison with massive QED$_3$ [45] helps explaining why an IR divergence occurs

for the one-loop damping rate, in contrast to the zero temperature case where the IR problem does not affect the dispersion equation, but only the residue of the propagator[33]. At this point, we should recall that the explicit solution that we have proposed here relies essentially on the 3-dimensional character of the dominant singularities. This has been widely recognized in relation with the infrared structure of thermal field theories [29], and, in the calculation of *static* quantities (like the free energy or the screening masses), it has been exploited in the method of "dimensional reduction" (see [41, 42, 43, 44] and references therein). We emphasize, however, that the damping rate is a dynamical quantity, and the usefulness of the dimensional reduction for this problem is not a priori obvious, given the subtleties of the analytic continuation from Matsubara to real external energy. If a dimensional reduction occurs in the computation of the large time behaviour, this is because of the particular IR behaviour of the magnetic photon propagator, as displayed in eqs. (2.16) or (2.29). The dynamical information which is contained in the later equations refers not only to the absence of the magnetic screening, but also to the phenomenon of Landau damping.

It is also worth emphasizing that our result takes into account only the most singular terms of the perturbative expansion. Because of the approximation used, we have lost control on the subleading terms. Although, in a strict perturbative sense, these are a priori less important, one cannot completely exclude the possibility that they may still modify our results in a qualitative way. It is hard to see however how they could destroy the quasiparticle picture, which we have shown to survive after a complete treatement of the leading IR divergences. Improvements of our solution may require an appropriate generalisation of the Bloch-Nordsieck model to finite temperature, a task that we have explored in this paper, but without reaching a definite conclusion. There are at least two points where the thermal BN model could possibly complete our previous analysis: the dynamical emergence of the upper cut-off $\sim gT$ (recall that, in the effective 3-dimensional theory, this cut-off has been introduced by hand), and, related to this, the consistent computation of the subleading terms beyond $\ln(\omega_p t)$ in eq. (4.13), that is, the terms of order $g^2 T$ which multiply the time in the exponent of $\Delta(t)$.

It is finally natural to ask what is the relevance of the present solution for the non-Abelian QCD plasma. It is widely believed that the self-interactions of the chromomagnetic gluons may generate magnetic screening at the scale $g^2 T$. As a crude model, we may include a screening mass $\mu \sim g^2 T$ in the magnetostatic propagator in

the QED calculation. Then eq. (3.42) provides, at very large times $t \gtrsim 1/g^2 T$, an exponential decay, $\Delta_\mu(t) \sim \exp(-\gamma t)$ with $\gamma = \alpha T \ln(\omega_p/\mu) = \alpha T \ln(1/g)$. However, in the physically more interesting regime of intermediate times $1/gT \ll t \ll 1/g^2 T$, the behavior is governed uniquely by the plasma frequency, according to our result (4.13): $\Delta_\mu(t) \sim \exp(-\alpha T t \ln \omega_p t)$. Thus, at least within this limited model, which is QED with a "magnetic mass", the time behavior in the physical regime remains controlled by the Bloch-Nordsieck mechanism. But, of course, this result gives no serious indication about the real situation in QCD, since it is unknown whether, in the present problem, the effects of the gluon self-interactions can be simply summarized in terms of a magnetic mass.

Acknowledgements

Appendix A

In this Appendix, we collect the sum rules for the photon spectral densities which are used in section 2.2.

The electric and magnetic spectral densities are defined in eq. (2.19) in terms of the corresponding propagators. In the hard thermal loop approximation, they involve both pole and cut pieces, as shown in eq. (2.22). They satisfy the following sum-rules[18], which trade the integrals over the off-shell spectral densities $\beta_{l,t}(q_0, q)$ for functions of $\omega_s(q)$ and $z_s(q)$:

$$
\begin{aligned}
\int_{-q}^{q} \frac{\mathrm{d}q_0}{2\pi q_0} \beta_l(q_0, q) &= \frac{1}{q^2} - \frac{1}{q^2 + m_D^2} - \frac{z_l(q)}{\omega_l^2(q)}, \\
\int_{-q}^{q} \frac{\mathrm{d}q_0}{2\pi q_0} \beta_t(q_0, q) &= \frac{1}{q^2} - \frac{z_t(q)}{\omega_t^2(q)}, \\
\int_{-q}^{q} \frac{\mathrm{d}q_0}{2\pi} q_0 \, \beta_t(q_0, q) &= 1 - z_t(q).
\end{aligned}
\tag{A.1}
$$

The first two of these sum rules are obtained by simply setting $\omega = 0$ in the spectral rep-

resentations (2.18), and by using $^*\Delta_l(0, q) = -1/(q^2 + m_D^2)$, $^*\Delta_t(0, q) = -1/q^2$, together with eq. (2.22). As for the third one, this is obtained by inserting eq. (2.22) into the familiar sum-rule

$$\int_{-\infty}^{\infty} \frac{dq_0}{2\pi} q_0 {}^*\rho_t(q_0, q) = 1, \qquad (A.2)$$

which is a consequence of the equal-time commutation relation for the quantum fields[13].

The use of the sum rules (A.1) is convenient to study both the ultraviolet and the infrared behavior of the q-integral in eq. (2.26). To this aim, we need the dispersion relations $\omega_{l,t}(q)$ [1, 2, 50] and the corresponding residues $z_{l,t}(q)$, which, in our conventions, read:

$$z_t = \frac{2\omega_t^2 (\omega_t^2 - q^2)}{3\omega_p^2\omega_t^2 - (\omega_t^2 - q^2)^2}, \qquad\qquad z_l = \frac{2\omega_l^2(\omega_l^2/q^2 - 1)}{3\omega_p^2 - (\omega_l^2 - q^2)}. \qquad (A.3)$$

At large momenta, $q \gg \omega_p$, we have the approximate expressions[50]

$$\omega_t^2(q) \simeq q^2 + 3\omega_p^2/2, \qquad\qquad \omega_l^2(q) \simeq q^2(1 + 4x_l(q)),$$

$$z_t(q) \simeq 1 - \frac{3\omega_p^2}{4q^2} \left(\ln \frac{8q^2}{3\omega_p^2} - 3 \right), \qquad\qquad z_l(q) \simeq \frac{8q^2}{3\omega_p^2} x_l(q), \qquad (A.4)$$

where

$$x_l(q) \equiv \exp\left(-\frac{2q^2}{3\omega_p^2} - 2 \right). \qquad (A.5)$$

From eqs. (A.1) and (A.4), we obtain, for $q \gg \omega_p$ (recall that $m_D^2 = 3\omega_p^2$),

$$\int_{-q}^{q} \frac{dq_0}{2\pi q_0} \beta_l(q_0, q) \simeq \frac{3\omega_p^2}{q^4},$$

$$\int_{-q}^{q} \frac{dq_0}{2\pi q_0} \left(1 - \frac{q_0^2}{q^2} \right) \beta_t(q_0, q) \simeq \frac{3\omega_p^2}{2q^4}. \qquad (A.6)$$

These estimates show that the integrand in eq. (2.26) behaves like ω_p^2/q^3 for momenta $q \gg \omega_p$.

We turn now to momenta $q \ll \omega_p$. We then have

$$\omega_t^2(q) \simeq \omega_p^2 + 6q^2/5, \qquad\qquad \omega_l^2(q) \simeq \omega_p^2 + 3q^2/5,$$

$$z_t(q) \simeq 1 - \frac{q^2}{5\omega_p^2}, \qquad\qquad z_l(q) \simeq \frac{\omega_p^2}{q^2} \left(1 + \mathcal{O}(q^4/\omega_p^4) \right), \qquad (A.7)$$

48

so that

$$\int_{-q}^{q} \frac{\mathrm{d}q_0}{2\pi q_0} \beta_l(q_0, q) \simeq \frac{4}{15} \frac{1}{\omega_p^2},$$

$$\int_{-q}^{q} \frac{\mathrm{d}q_0}{2\pi q_0} \beta_t(q_0, q) \simeq \frac{1}{q^2} - \frac{1}{\omega_p^2},$$

$$\int_{-q}^{q} \frac{\mathrm{d}q_0}{2\pi} q_0 \, \beta_t(q_0, q) \simeq \frac{1}{5\omega_p^2}. \tag{A.8}$$

When these expressions are inserted in eq. (2.26), the contribution in $1/q^2$ of the magnetic spectral function (the second line in eq. (A.8)) generates a logarithmic IR singularity.

Appendix B

Since there is no phase-space available for the direct decay of the on-shell fermion into a pair of massless particles, one expects that the damping rate computed from the *bare* one-loop fermion self-energy should vanish. However, at finite temperature, this argument is complicated by infrared singularities which arise because of the enhancement of collinear singularities by the Bose-Einstein thermal factor.

To illustrate this problem, we consider the calculation of the damping rate to bare one-loop order in the Coulomb gauge. This is obtained by simply replacing, in eq. (2.21), the photon spectral functions with their bare counterparts, namely $\rho_l^{(0)} = 0$ and $\rho_t^{(0)}(q_0, q) = \rho_0(q_0, q)$, with ρ_0 from eq. (1.2). In the on-shell limit, the whole contribution to γ comes from space-like photons, with $|q_0| \leq q$. However, since the free spectral density (1.2) has support precisely at the integration limits $q_0 = \pm q$, we should be more careful when evaluating eq. (2.21) in the on-shell limit $\omega \to p$. For ω close to, but different from, p, the latter equation yields (compare with eq. (2.25))

$$\gamma_0(\omega \simeq p) \simeq \pi g^2 T \int \frac{\mathrm{d}^3 q}{(2\pi)^3} \int_{-\infty}^{\infty} \frac{\mathrm{d}q_0}{2\pi q_0} \delta(\omega - p - q_0 + q\cos\theta)(1 - \cos^2\theta)\rho_0(q_0, q). \tag{B.1}$$

After the angular integration, we obtain

$$\gamma_0(\omega \simeq p) \simeq \frac{g^2 T}{8\pi}(\omega - p) \int_0^{\infty} \frac{\mathrm{d}q}{q^2} \int_{\omega-p-q}^{\omega-p+q} \frac{\mathrm{d}q_0}{q_0} (2q_0 - (\omega - p))\Big[\delta(q_0 - q) - \delta(q_0 + q)\Big]$$

$$= \frac{g^2 T}{4\pi} |\omega - p| \int_{|\omega-p|/2}^{\infty} \frac{\mathrm{d}q}{q^2} \left(1 - \frac{|\omega - p|}{2q}\right). \tag{B.2}$$

If we let now $\omega \to p$, the factor in the front of the last integral goes to zero, but the integral itself becomes IR divergent. An explicit calculation shows that the r.h.s. of eq. (B.2) is in fact independent of $(\omega - p)$, and equals

$$\gamma_0 = \frac{g^2 T}{4\pi}. \tag{B.3}$$

This result is, however, unphysical. It arises from the emission or the absorbtion of *collinear* ($\theta = 0$, $q_0 = q$ or, respectively, $\theta = \pi$, $q_0 = -q$) massless photons, whose contributions are enhanced by the Bose-Einstein factor T/q_0. Such contributions do not survive screening corrections. However, since the gauge-dependent terms in the photon propagator are not modified by the plasma effects, they may generate — by the mechanism alluded to before — a non-vanishing contribution to the on-shell self-energy [51]. Note that an entirely similar problem arises in the three-dimensional gauge theories at zero-temperature, when computing the dispersion equation to one loop order[45].

To overcome this problem, it has been suggested [45, 40] to take the on-shell limit in the presence of an IR regulator, say, an IR cut-off μ. With such a cut-off, the q-integral in eq. (B.2) remains finite as $\omega \to p$, and the total result for $\gamma_0(\omega = p)$ vanishes. Thus, the damping rate remains zero at the bare one-loop level, as expected. In the same way one verifies that the dispersion relation is gauge-independent, as it should[39]. On the other hand, the residue of the propagator at the mass-shell becomes dependent on the IR cut-off μ, and (linearly) divergent as $\mu \to 0$.

Appendix C

We verify here, on an explicit two-loop calculation, some general features of the infrared behavior of the on-shell self-energy in perturbation theory. Specifically, we shall show that the leading divergences are power-like, and can be fully taken into account by restricting all the internal Matsubara sums to their zero frequency photon modes.

At two loop order, the fermion self-energy is given by the two diagrams in Fig. 11, which yield

$$\Sigma^{(2)}(p) = -(g^2 T)^2 \sum_{q^0 = i\omega_m} \sum_{k^0 = i\omega_r} \int \frac{\mathrm{d}^3 q}{(2\pi)^3} \int \frac{\mathrm{d}^3 k}{(2\pi)^3} \; \gamma_\mu S_0(p+q) \gamma_\rho S_0(p+q+k)$$
$$\left[\gamma_\lambda S_0(p+q) \gamma_\nu + \gamma_\nu S_0(p+k) \gamma_\lambda \right] {}^* D^{\mu\nu}(q) \, {}^* D^{\rho\lambda}(k) \,. \tag{C.1}$$
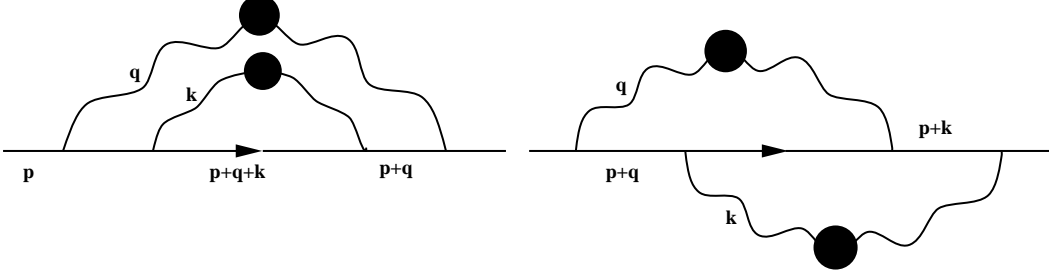
Figure 11: Two-loop diagrams for the fermion self-energy.

The notations here are as in eq. (2.17); for instance, $p^0 = i\omega_n = i(2n+1)\pi T$, $q^0 = i\omega_m = i2\pi mT$ and $k^0 = i\omega_r = i2\pi rT$, with integers n, m and r. According to eq. (1.6), the correction to the positive mass-shell is determined by the function $\Sigma_+(\omega, p) = \mathrm{tr}\left(h_\pm(\hat{\mathbf{p}})\Sigma(\omega, \mathbf{p})\right)/2$. As $\omega \simeq p$, the most singular contributions to Σ_+ are obtained by using the effective Feynman rules described at the end of section 3.1. At two loop level, this amounts to replacing eq. (C.1) by

$$
\Sigma_+^{(2)}(p) = -(g^2 T)^2 \sum_{q^0 = i\omega_m} \sum_{k^0 = i\omega_r} \int \frac{\mathrm{d}^3 q}{(2\pi)^3} \int \frac{\mathrm{d}^3 k}{(2\pi)^3} \, G_0(p+q) \, G_0(p+q+k)
$$
$$
\left[G_0(p+q) + G_0(p+k) \right] \tilde{D}(q) \, \tilde{D}(k) \,, \tag{C.2}
$$

where $\tilde{D}(q) \equiv v^{i\,*} D^{ij}(q) v^j$ is the (HTL resummed) propagator of the magnetic photon. (We recall that the electric propagator does not yield IR singularities.) Eq. (C.2) is precisely the two-loop self-energy in the Bloch-Nordsieck approximation.

The Matsubara sums over ω_m and ω_r are conveniently performed by contour methods, and by using the spectral representation (2.18) of $^*\Delta_t(q)$. In doing this, one gets several terms, corresponding to the poles of the various propagators in the complex planes q^0 and k^0. Every such a term involves three energy denominators, and the product of two statistical factors. The latter are either of the bosonic or of the fermionic type, according to whether they correspond to poles of a photon propagator, or of an electron propagator, respectively. When the external energy approaches the tree-level mass-shell, $\omega \to p \equiv \mathbf{v} \cdot \mathbf{p}$, all the energy denominators are soft, of the type $1/(q_0 - \mathbf{v} \cdot \mathbf{q})$, and may give infrared problems. (The hard energy denominators, which were potentially present in the full two-loop self-energy (C.1), have been eliminated by the simplified Feynman rules leading to eq. (C.2).) Then, the *leading* IR singularities arise uniquely from the terms which involve the product of *two Bose-Einstein distribution functions*, since $N(q^0)N(k^0) \simeq T^2/(q^0 k^0)$ at soft momenta. By isolating these most singular terms, we obtain, after a straightforward

51

calculation,

$$\Sigma_+^{(2)}(\omega \simeq p) \;\simeq\; (g^2 T)^2 \int \frac{\mathrm{d}^3 q}{(2\pi)^3} \int \frac{\mathrm{d}^3 k}{(2\pi)^3} \int_{-\infty}^{\infty} \frac{\mathrm{d}q_0}{2\pi q_0} \, {}^*\!\rho_t(q_0, q) \int_{-\infty}^{\infty} \frac{\mathrm{d}k_0}{2\pi k_0} \, {}^*\!\rho_t(k_0, k)$$

$$\frac{1}{\omega + q_0 - \mathbf{v} \cdot (\mathbf{p} + \mathbf{q})} \frac{1}{\omega + q_0 + k_0 - \mathbf{v} \cdot (\mathbf{p} + \mathbf{q} + \mathbf{k})}$$

$$\left[\frac{1}{\omega + q_0 - \mathbf{v} \cdot (\mathbf{p} + \mathbf{q})} + \frac{1}{\omega + k_0 - \mathbf{v} \cdot (\mathbf{p} + \mathbf{k})} \right] , \tag{C.3}$$

where it is understood that the external energy carries a small positive imaginary part $(\omega \to \omega + i\eta)$.

The energy integrals over q_0 and over k_0 involve both the pole and the cut pieces of the photon spectral density. However, it is only the off-shell (or cut) piece of ${}^*\!\rho_t$ which yields a singular contribution, so we may as well restrict the aforementioned energy integrals to space-like momenta, $|q_0| \le q$ and $|k_0| \le q$, and replace the full spectral functions by β_t. Then, the subsequent analysis follows closely the discusion of the (resummed) one-loop self-energy in section 2.2. The singular domain is that of very soft photon momenta, $q, k \ll gT$, where we can use eq. (2.29) to replace $\beta_t(q_0 \ll q)/q_0$ by $(2\pi/q^2)\delta(q_0)$. At the same time, we have to supplement the momentum integrations with an upper cut-off of the order of $\omega_p \sim gT$. The net effect is that the leading singular piece of $\Sigma_+^{(2)}(\omega \simeq p)$ is the same as it would be obtained by retaining only the static terms $\omega_m = \omega_r = 0$ in the Matsubara sums of eq. (C.2). That is,

$$\Sigma_+^{(2)}(\omega \simeq p) \;\simeq\; (g^2 T)^2 \int \frac{\mathrm{d}^3 q}{(2\pi)^3} \frac{1}{q^2} \int \frac{\mathrm{d}^3 k}{(2\pi)^3} \frac{1}{k^2} \frac{1}{\omega - \mathbf{v} \cdot (\mathbf{p} + \mathbf{q} + \mathbf{k})}$$

$$\frac{1}{\omega - \mathbf{v} \cdot (\mathbf{p} + \mathbf{q})} \left[\frac{1}{\omega - \mathbf{v} \cdot (\mathbf{p} + \mathbf{q})} + \frac{1}{\omega - \mathbf{v} \cdot (\mathbf{p} + \mathbf{k})} \right] . \tag{C.4}$$

Since this is divergent as $\omega \to \mathbf{v} \cdot \mathbf{p}$, we take the mass-shell limit in the presence on an IR cut-off μ, and obtain

$$\Sigma_+^{(2)}(\omega \simeq p) \simeq -(g^2 T)^2 \int \frac{\mathrm{d}^3 q}{(2\pi)^3} \frac{1}{q^2} \frac{1}{(\mathbf{v} \cdot \mathbf{q} - i\eta)^2} \int \frac{\mathrm{d}^3 k}{(2\pi)^3} \frac{1}{k^2} \frac{1}{\mathbf{v} \cdot \mathbf{k} - i\eta} \;=\; i \frac{2}{\pi} \frac{(\alpha T)^2}{\mu} \ln \frac{\omega_p}{\mu} . \tag{C.5}$$

We thus find the linear plus logarithmic infrared divergence mentioned in section 2.3.

According to eq. (2.33), the computation of $\gamma^{(2)}$ — the two-loop contribution to the damping rate — requires also the one-loop residue, $z^{(1)}(p) - 1 = (\partial \Sigma_+^{(1)} / \partial \omega)$. Similarly to eq. (C.4), we obtain the leading IR-singular contribution to $\Sigma_+^{(1)}$ in the form

$$\Sigma_+^{(1)}(\omega, p) \;\simeq\; g^2 T \int \frac{\mathrm{d}^3 q}{(2\pi)^3} \frac{1}{q^2} \frac{1}{\omega - \mathbf{v} \cdot (\mathbf{p} + \mathbf{q}) + i\eta} , \tag{C.6}$$

and thus

$$z^{(1)}(p) - 1 \simeq -g^2 T \int \frac{\mathrm{d}^3 q}{(2\pi)^3} \frac{1}{q^2} \frac{1}{(\mathbf{v} \cdot \mathbf{q} - i\eta)^2} \simeq \frac{2}{\pi} \frac{\alpha T}{\mu}, \tag{C.7}$$

in the presence of the IR regulator. The linear IR divergence of the residue compensates the dominant singularity of the two-loop self-energy (C.5), so that the leading contribution to $\gamma^{(2)}$ — which remains beyond the accuracy of the present computation — is of the order $(\alpha^2 T^2/\omega_p)(\ln(\omega_p/\mu))^2 \sim g^3 T(\ln(\omega_p/\mu))^2$. Even if still divergent as $\mu \to 0$, this does not contribute to the order $g^2 T$ which is our concern here.

Let us finally provide an all order argument for the cancellation of the strongest, power-like, infrared divergences in the perturbative evaluation of γ. To this aim, we consider the Dyson-Schwinger equation for the fermion self-energy within the effective three-dimensional Bloch-Nordsieck theory:

$$\Sigma(\omega, \mathbf{p}) = -g^2 T \int \frac{\mathrm{d}^3 q}{(2\pi)^3} \, v^i \, S(\omega, \mathbf{p} + \mathbf{q}) \, \Gamma^j(\mathbf{p} + \mathbf{q}, \mathbf{p}) \, D_0^{ij}(\mathbf{q}), \tag{C.8}$$

where $D_0^{ij}(\mathbf{q}) = \delta^{ij}/q^2$, S is the full BN propagator,

$$S(\omega, \mathbf{p} + \mathbf{q}) = \frac{-1}{\omega - \mathbf{v} \cdot (\mathbf{p} + \mathbf{q}) - \Sigma(\omega, \mathbf{p} + \mathbf{q})}, \tag{C.9}$$

and $\Gamma^j(\mathbf{p} + \mathbf{q}, \mathbf{p})$ is the full vertex, which is related to S via the Ward identity

$$q^j \, \Gamma_j(\mathbf{p} + \mathbf{q}, \mathbf{p}) = S^{-1}(\omega, \mathbf{p} + \mathbf{q}) - S^{-1}(\omega, \mathbf{p}). \tag{C.10}$$

We make now the usual assumption [53] that the dominant IR behavior involves only the longitudinal piece of the vertex. This is entirely determined by the Ward identity:

$$\Gamma^j(\mathbf{p} + \mathbf{q}, \mathbf{p}) = \frac{v^j}{\mathbf{v} \cdot \mathbf{q}} \left[S^{-1}(\omega, \mathbf{p} + \mathbf{q}) - S^{-1}(\omega, \mathbf{p}) \right]. \tag{C.11}$$

When inserted in eq. (C.8), this yields

$$\Sigma(\omega, \mathbf{p}) \simeq -g^2 T \int \frac{\mathrm{d}^3 q}{(2\pi)^3} \frac{1}{q^2} \frac{1}{\mathbf{v} \cdot \mathbf{q} - i\eta} \left[1 - S^{-1}(\omega, \mathbf{p}) \, S(\omega, \mathbf{p} + \mathbf{q}) \right]. \tag{C.12}$$

As already explained, eq. (C.8) reproduces the most singular terms of the perturbative expansion, and this remains true after inserting the approximation (C.11) for the vertex function, as can be verified explicitly by developing eq. (C.12) in perturbation theory. We now take the on-shell limit in the presence of an IR cut-off μ, taken as a small photon mass. As long as $\mu \neq 0$, there is no IR problem, and we expect the mass-shell to correspond

to a simple pole of the exact propagator. Thus, $S^{-1}(\omega, \mathbf{p})$ vanishes on shell, and the second term in eq. (C.12) gives no contribution. The leading contribution to the on-shell self-energy reads then

$$\Sigma(\text{on} - \text{shell}) \simeq -g^2 T \int \frac{\mathrm{d}^3 q}{(2\pi)^3} \frac{1}{q^2 + \mu^2} \frac{1}{\mathbf{v} \cdot (\mathbf{q}) - i\eta} \simeq i \frac{g^2 T}{4\pi} \ln \frac{\omega_p}{\mu}, \qquad (\text{C.13})$$

and coincides with the IR singular part of the one-loop self-energy. This is only possible if the aforementioned compensation of the leading power-like divergences holds in all orders. Note that the above arguments become meaningless in the physical limit $\mu \to 0$, where not only does the estimate (C.13) become logarithmically divergent, but the integral multiplying $S^{-1}(\omega, \mathbf{p})$ also diverges on the mass-shell.

References

[1] O.K. Kalashnikov and V.V. Klimov, Sov. J. Nucl. Phys. **31** (1980) 699; V.V. Klimov, Sov. J. Nucl. Phys. **33** (1981) 934; Sov. Phys. JETP **55** (1982) 199.

[2] H.A. Weldon, Phys. Rev. **D26** (1982) 1394; Phys. Rev. **D26** (1982) 2789.

[3] R.D. Pisarski, Phys. Rev. Lett.**63** (1989) 1129.

[4] E. Braaten and R.D. Pisarski, Phys. Rev. Lett.**64** (1990) 1338; Phys. Rev. **D42** (1990) 2156; Nucl. Phys. **B337** (1990) 569.

[5] J. Frenkel and J.C. Taylor, Nucl. Phys. **B334** (1990) 199; J.C.Taylor and S.M.H.Wong, Nucl. Phys. **B346** (1990) 115.

[6] G. Baym, H. Monien, C.J. Pethick, and D.G. Ravenhall, Phys. Rev. Lett.**64** (1990) 1867.

[7] E. Braaten and M.H. Thoma, Phys. Rev. **D44** (1991) 1298.

[8] R. Kobes, G. Kunstatter and K. Mak, Phys. Rev. **D45** (1992) 4632; E. Braaten and R. Pisarski, Phys. Rev. **D46** (1992) 1829.

[9] R. Efraty and V.P. Nair, Phys. Rev. Lett.**68** (1992) 2891; Phys. Rev. **D47** (1993) 5601; R. Jackiw and V.P. Nair, Phys. Rev. **D48** (1993) 4991.

[10] J.P. Blaizot and J.-Y. Ollitrault, Phys. Rev. **D48** (1993) 1390.

[11] J.P. Blaizot and E. Iancu, Nucl. Phys. **B390** (1993) 589; Phys. Rev. Lett.**70** (1993) 3376; Nucl. Phys. **B417** (1994) 608; Phys. Rev. Lett.**72** (1994) 3317; Nucl. Phys. **B421** (1994) 565.

[12] J.P. Blaizot, J.-Y. Ollitrault and E. Iancu, *Collective Phenomena in the Quark-Gluon Plasma*, in *Quark-Gluon Plasma 2*, Editor R.C. Hwa (World Scientific, 1996).

[13] M. Le Bellac, *Recent Developments in Finite Temperature Quantum Field Theories*, (Cambridge University Press, 1996).

[14] L.Kadanoff and G.Baym, *Quantum Statistical Mechanics*, (Benjamin, New York,1962).

[15] V.V. Lebedev and A.V. Smilga, Phys. Lett. **B253** (1991) 231; Ann. Phys.**202** (1990) 229; Physica **A181** (1992) 187.

[16] C.P. Burgess and A.L. Marini, Phys. Rev. **D45** (1992) R17; A.K. Rebhan, Phys. Rev. **D46** (1992) 482.

[17] R. Baier, H. Nakkagawa and A. Niégawa, Can. J. Phys. **71** (1993) 205.

[18] R.D. Pisarski, Phys. Rev. **D47** (1993) 5589.

[19] T. Altherr, E. Petitgirard and T. del Rio Gaztelurrutia, Phys. Rev. **D47** (1993) 703.

[20] H. Heiselberg and C.J. Pethick, Phys. Rev. **D47** (1993) R769.

[21] S. Peigné, E. Pilon and D. Schiff, Z. Phys. **C60** (1993) 455.

[22] R. Baier and R. Kobes, Phys. Rev. **D50** (1994) 5944.

[23] A.V. Smilga, Phys. Atom. Nuclei **57** (1994) 519.

[24] A. Niégawa, Phys. Rev. Lett.**73** (1994) 2023.

[25] F. Flechsig, H. Schulz and A.K. Rebhan, Phys. Rev. **D52** (1995) 2994.

[26] U. Kraemmer, A. Rebhan and H. Schulz, Ann. Phys.**238** (1995) 286.

[27] R.D. Pisarski, Nucl. Phys. **A525** (1991) 175.

[28] M.H. Thoma, Phys. Rev. **D51** (1995) 862.

[29] A. Linde, Phys. Lett. **B96** (1980) 289; D.J. Gross, R.D. Pisarski and L.G. Yaffe, Rev. Mod. Phys. **53** (1981) 43.

[30] E. Fradkin, Proc. Lebedev Phys. Inst. **29** (1965) 7; J.P. Blaizot, E. Iancu and R. Parwani, Phys. Rev. **D52** (1995) 2543.

[31] J.P. Blaizot and E. Iancu, Phys. Rev. Lett.**76** (1996) 3080.

[32] F. Bloch and A. Nordsieck, Phys. Rev.**52** (1937) 54.

[33] N.N. Bogoliubov and D.V. Shirkov, *Introduction to the Theory of Quantized Fields* (Interscience Publishers, inc, New-York, 1959).

[34] H.A. Weldon, Phys. Rev. **D44** (1991) 3955; Phys. Rev. **D49** (1994) 1579.

[35] K. Takashiba, *Thermal two point function of a heavy muon in hot QED plasma within Bloch Nordsieck Approximation*, hep-ph 9501223 (unpublished).

[36] H.A. Weldon, Phys. Rev. **D28** (1983) 2007.

[37] R.L. Kobes and G.W. Semenoff, Nucl. Phys. **B260** (1985) 714; Nucl. Phys. **B272** (1986) 329.

[38] J.D. Bjorken and S.D. Drell, *Relativistic Quantum Mechanics* (McGraw-Hill, Inc., 1964).

[39] R. Kobes, G. Kunstatter and A. Rebhan, Phys. Rev. Lett.**64** (1990) 2992; Nucl. Phys. **B355** (1991) 1.

[40] A.K. Rebhan, Phys. Rev. **D46** (1992) 4779.

[41] S. Nadkarni, Phys. Rev. **D27** (1983) 917; Phys. Rev. **D38** (1988) 3287.

[42] E. Braaten, Phys. Rev. Lett.**74** (1995) 2164; E. Braaten and A. Nieto, Phys. Rev. **D51** (1995) 6990.

[43] K. Farakos, K. Kajantie, K. Rummukainen and M. Shaposhnikov, Nucl. Phys. **B425** (1994) 67; K. Kajantie, M. Laine K. Rummukainen and M. Shaposhnikov, Nucl. Phys. **B458** (1996) 90.

[44] J.P. Blaizot and E. Iancu, Nucl. Phys. **B459** (1996) 559.

[45] D. Sen, Phys. Rev. **D41** (1990) 1227.

[46] S. Weinberg, *The Quantum Theory of Fields* (Cambridge University Press, 1995).

[47] E. Braaten and R.D. Pisarski, Nucl. Phys. **B339** (1990) 310.

[48] E. Braaten and R. Pisarski, Phys. Rev. **D45** (1992) 1827; J. Frenkel and J.C. Taylor, Nucl. Phys. **B374** (1992) 156.

[49] E.M. Lifshitz and L.P. Pitaevskii, *Physical Kinetics*, (Pergamon Press, Oxford, 1981).

[50] R.D. Pisarski, Physica **A158** (1989) 146.

[51] R. Baier, G. Kunstatter and D. Schiff, Phys. Rev. **D45** (1992) 4381; Nucl. Phys. **B388** (1992) 287.

[52] A.K. Rebhan, private communication.

[53] J.S. Ball and T.-W. Chiu, Phys. Rev. **D22** (1980) 2542; Phys. Rev. **D22** (1980) 2550.